



1-C

2-8



2-5

3-15



2-2

3-5



2-0

4-0



1-8

4-5



1-1



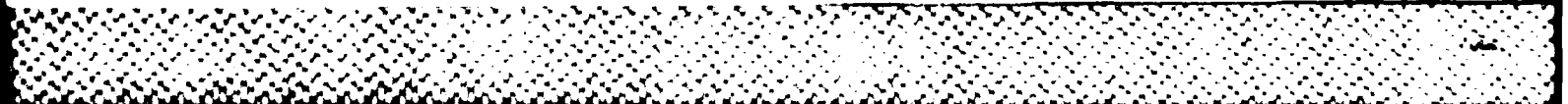
1-25



1-4



1-6



2

AD-A187 961



Electrical Engineering Department

UNIVERSITY OF MARYLAND, COLLEGE PARK, MD 20742

Annual Report on Contract N0001484K0550
Microwave Absorption Characteristics of DNA

Prepared by

Christopher C. Davis

Professor

Electrical Engineering Department

University of Maryland

College Park, Maryland 20742

period covered by report 8-1-85 to 7-31-86

DISTRIBUTION STATEMENT A
Approved for public release
Distribution Unlimited

DTIC
ELECTE
NOV 16 1987
S D E



COLLEGE OF ENGINEERING GLENN L. MARTIN INSTITUTE OF TECHNOLOGY

REPORT DOCUMENTATION PAGE

Form Approved
OMB No 0704-0188

| | | | |
|--|--|---|--------------------------|
| 1a REPORT SECURITY CLASSIFICATION (U) | | 1d RESTRICTIVE MARKINGS NA | |
| 2a SECURITY CLASSIFICATION AUTHORITY NA | | 3 DISTRIBUTION/AVAILABILITY OF REPORT Distribution Unlimited | |
| 2b DECLASSIFICATION/DOWNGRADING SCHEDULE NA | | 5 MONITORING ORGANIZATION REPORT NUMBER(S) | |
| 4 PERFORMING ORGANIZATION REPORT NUMBER(S) NA | | 7a NAME OF MONITORING ORGANIZATION Office of Naval Research | |
| 6a NAME OF PERFORMING ORGANIZATION University of Maryland College Park | 6b OFFICE SYMBOL (if applicable) | 7b ADDRESS (City, State, and ZIP Code) 800 N. Quincy Street, Arlington, VA 22217-5000 | |
| 6c ADDRESS (City, State, and ZIP Code) Electrical Engineering Department University of Maryland, College Park, MD20742 | | 9 PROCUREMENT INSTRUMENT IDENTIFICATION NUMBER N0001484K0550 | |
| 8a NAME OF FUNDING SPONSORING ORGANIZATION Office of Naval Research | 8b OFFICE SYMBOL (if applicable) ONR | 10 SOURCE OF FUNDING NUMBERS | |
| 6c ADDRESS (City, State, and ZIP Code) 800 N. Quincy Street Arlington, VA 22217-5000 | | PROGRAM ELEMENT NO 61153N | PROJECT NO RR04108 |
| | | TASK NO 4414411 | WORK UNIT ACCESSION NO |
| 11 TITLE (Include Security Classification) Microwave Absorption Characteristics of DNA | | | |
| 12 PERSONAL AUTHOR(S) Christopher C. Davis | | | |
| 13a TYPE OF REPORT Annual | 13b TIME COVERED FROM 8/1/85 TO 7/31/86 | 14 DATE OF REPORT (Year, Month, Day) 10/14/87 | 15 PAGE COUNT 54 |
| 16 SUPPLEMENTARY NOTATION NA | | | |
| 17 COSATI CODES | | 18 SUBJECT TERMS (Continue on reverse if necessary and identify by block number) | |
| FIELD | GROUP | SUB-GROUP | |
| 08 | | | |
| | | Microwave Absorption, DNA, Dielectrometry Ultrasonic Absorption | |
| 19 ABSTRACT (Continue on reverse if necessary and identify by block number) | | | |
| <p>This report describes work in four areas:</p> <ol style="list-style-type: none"> 1. Continuing studies of the microwave absorption characteristics of DNA, including further investigation of the open-probe technique as a means for making such measurements. 2. Studies of the effect of microwaves on plasmid DNA. 3. Ultrasonic absorption properties of biomaterials. 4. An investigation of cell shape deformation in strong AC electric fields. | | | |
| 20 DISTRIBUTION/AVAILABILITY OF ABSTRACT <input checked="" type="checkbox"/> UNCLASSIFIED UNLIMITED <input type="checkbox"/> SAME AS RPT <input type="checkbox"/> DTIC USERS | | 21 ABSTRACT SECURITY CLASSIFICATION (U) | |
| 22a NAME OF RESPONSIBLE INDIVIDUAL Dr. J.A. Maide | | 22b TELEPHONE NUMBER (Area Code) (202)696-4055 | 22c OFFICE SYMBOL ONR |

ABSTRACT

This report describes work in four areas:

1. Continuing studies of the microwave absorption characteristics of DNA, including further investigation of the open-probe technique as a means for making such measurements.
2. Studies of the effect of microwaves on plasmid DNA.
3. Ultrasonic absorption properties of biomaterials.
4. An investigation of cell shape deformation in strong AC electric fields.

| | |
|--------------------|-------------------------------------|
| Accession For | |
| NTIS GRA&I | <input checked="" type="checkbox"/> |
| DTIC TAB | <input type="checkbox"/> |
| Unannounced | <input type="checkbox"/> |
| Justification | |
| By _____ | |
| Distribution/ | |
| Availability Codes | |
| Dist | Avail and/or Special |
| A-1 | |



INTRODUCTION

During the reporting period several projects were in progress

- (1) Continuing investigation of the microwave absorption characteristics of plasmid DNA
- (2) Studies of the effect of microwaves on plasmid DNA
- (3) Ultrasonic absorption studies of biomaterials
- (4) An investigation of cell shape deformation in strong electric fields.

The work carried out and the results obtained will be described separately for each study.

MICROWAVE ABSORPTION STUDIES

For the last several years we have been studying the microwave absorption characteristics of various forms of DNA in solution. This work has been described in detail elsewhere [1-6]. Although we have used several geometries for our sample holders the one that we have favored in recent years has been the *open-probe* geometry [7-9]. This method has several advantages in biological applications. It is biocompatible, as the undesirable exposure of samples to metal ions can be avoided, it does not require an excessive amount of sample, and expensive samples can be recovered intact for further biochemical assay after microwave measurements. During the reporting period we received funding from ONR to allow upgrade of our measurement system to a Hewlett-Packard 8510 network analyzer from the 8410 system we had used for the last several years. However, the 8510 system was not delivered and installed during the period under discussion here so our observations continued to be made on the 8410 system described previously [5].

To conclude our observations on the 8410 system we made a very careful re-investigation of the open-probe technique. This technique has been the subject of much discussion regarding accuracy, repeatability, and introduction of artifacts into measured data. We ran a series of measurements on known molarity saline solutions to test

- (i) absolute measurement accuracy
- (ii) repeatability
- (iii) the effect of sample volume
- (iv) the possibility of artifacts in data.

Examples of results from these measurements will be presented later, but in summary, several conclusions can be drawn:

- When the calibration technique described by Kraszewski, Stuchly and Stuchly [10] is used, which involves calibration with known test solutions *at the reference plane of the end of the probe*, artifactual resonant structure is *not* introduced into the data. Although the absolute accuracy of measured data can deviate by several percent from theoretical values obtained from the Debye equation, the deviation, when it occurs, is monotonous.
- Comparison of one solution with another is reliably accomplished.
- It is possible to introduce resonant, artifactual structure into measured data if the network analyzer is calibrated at its reference connector in the standard way, using a short, open, and sliding load, and the probe is subsequently connected. We have *never* used this technique, it does not vector-error-correct away the reflections between the probe end and the calibration reference plane connector.

Open-Probe Technique

The open-probe technique lends itself to reliable implementation with the latest generation of computer-controlled network analyzers. This technique is flexible, offers easy biocompatibility, and can be used with small quantities of sample. For highest accuracy the technique works best at low microwave frequencies, but can provide acceptable accuracy even to 12GHz. The relative dielectric properties of different materials can be monitored reliably and repeatably.

There are many ways for measuring the dielectric properties of materials. However, most measurements are made, in essence, by taking a sample of controlled, simple geometry, irradiating it and measuring the incident, reflected and transmitted radiation. These measurements can be measurements of intensity, or of the amplitude and phase of the electric fields. There are also methods in which the change in Q of a resonator when it is loaded with sample are used to determine its dielectric parameters. However, this technique is most easily applied to low-loss materials so has not been extensively used for measurements of biological materials. These materials frequently have a large water content and are, therefore, intrinsically very lossy. Information about dielectric parameters can also be obtained, indirectly, by directly measuring the microwave absorption coefficient.

From a practical point of view, dielectric properties involve samples contained within rectangular waveguides. Solid samples can be machined into slabs to fit inside the waveguide. The samples must be bounded within the waveguide, for example by a thin Teflon washer and a short circuit, as shown in Fig. (1).

In this geometry the complex reflection coefficient of the sample at the *reference* plane is

$$\Gamma = \frac{Z^* \tanh 2\gamma d - 1}{Z^* \tanh 2\gamma d + 1} \quad (1)$$

where γ is the propagation constant in the sample and $Z^* = \sqrt{\mu_r/\epsilon_r^*}$ is the normalized impedance of the waveguide when it is filled with sample.

Eq. (1) can be solved numerically for the complex dielectric constant ϵ_r^* . The complex permittivity of the sample is

$$\epsilon^* = \epsilon_0 \epsilon_r^* = \epsilon_0(\epsilon' - i\epsilon'') \quad (2)$$

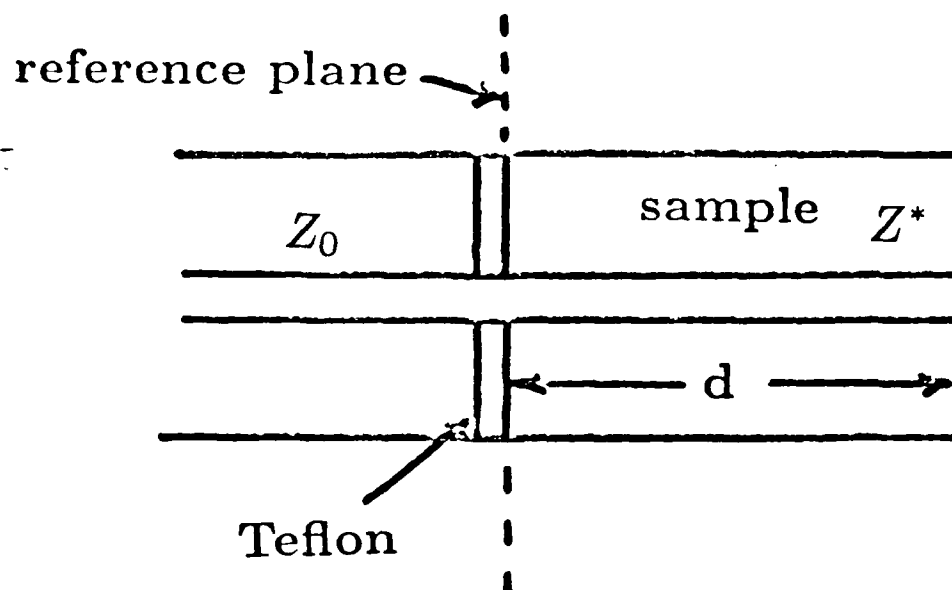
From ϵ' and ϵ'' , the plane-wave intensity absorption coefficient α can be determined

$$\alpha = \frac{2\pi f}{c_0} \sqrt{2\epsilon' \sqrt{1 + (\epsilon''/\epsilon')^2} - 2\epsilon'} \quad (3)$$

To achieve highest accuracy in solving Eq. (1) the length of the sample must be constrained to be close to an odd number of quarter guide wavelengths [3].

Stuchly and Stuchly [11] have discussed in detail the advantages and disadvantages of the various geometrical arrangements that can be used for dielectric measurements in waveguides. However, when measurements of biological materials must be made, there are other constraints that can limit the choice of geometry. The waveguide sample holder must be biocompatible, this can eliminate any sample holder where the biomaterial is in contact with inappropriate metals. For example, dissolved copper can cause structural damage to plasmid DNA in solution [12]. Also, for biomaterials that can only be obtained in small amounts, because they are difficult or expensive to produce in quantity, the measurement technique should allow recovery of the sample without contamination, and not require a large volume of sample. The one technique that meets these criteria, and which does not require any special sample fabrication is the open-probe technique. A typical open-probe is a length of rigid, miniature coaxial cable machined flush at one end and with an appropriate coaxial connector on the other. The center

Coaxial line terminated with short circuit



reflection coefficient

$$\Gamma = \frac{Z^* \tanh 2\gamma d - 1}{Z^* \tanh 2\gamma d + 1}$$

γ is propagation constant in sample

$Z^* = \sqrt{\frac{\mu_r}{\epsilon_r}}$ is normalized impedance

Fig. 1. Geometry for measurement of dielectric properties of a material contained in a section of shorted waveguide.

conductor of the coax should not protrude. The probe can be fabricated with a ground plane, but this is not essential, particularly when measurements on high-loss material are made. If the complex reflection coefficient at the end of the probe when it is immersed in a sample can be measured, then the dielectric parameters can be determined. The equivalent circuit of the probe is shown in Fig. (2).

The capacitance C_0 results from fringing fields beyond the end of the probe, C_f results from evanescent modes that propagate back up the coax after being excited by the mismatch at the probe tip. The term in G_0 results from radiation into the sample and can be neglected provided $a/\lambda \ll 1$, where a is the inner radius of the outer conductor of the coax, and λ is the wavelength in the sample [8]. For 3.6mm rigid coax in water at 10 GHz $a/\lambda = 0.134$. The reflection coefficient at the probe tip is

$$\Gamma = \frac{1 - Y^*}{1 + Y^*} \quad (4)$$

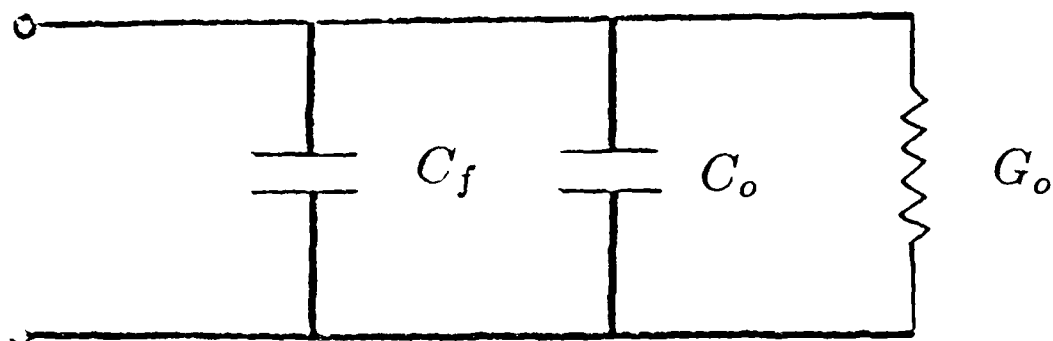
where

$$Y^* = i\omega C_f Z_0 + i\omega C_0 Z_0 \epsilon_r^* + G_0 Z_0 (\epsilon_r^*)^{5/2} \quad (5)$$

If Y^* , C_f , C_0 and G_0 , which are all dependent on frequency, can be determined, then so can ϵ_r^* .

There has been considerable debate whether the open-probe technique can be implemented in practice in a reliable way. We have made extensive measurements, over a frequency range from 1 to 12 GHz using standard dielectric fluids, different probe geometries, and with different volumes of sample to resolve this discussion. Our measurements are made with a computer-controlled network analyzer described elsewhere [5]. We perform a one-port S_{11} calibration at the open probe tip using the technique described by Kraszewski et al [10]. The scattering parameters of the error network, which contains all the imperfections and non-ideal behavior of the microwave measurement system up to the probe tip, are determined by measurement of a short circuit, measurement of the open probe, and measurement with the probe immersed in a standard liquid. The standard liquid used should, ideally, have dielectric properties close to the material that is to be measured. We use saline solutions from 0.1M to 1.0M and calculate the values of ϵ_r^* from the Debye equation. Equations (4) and (5) are used in calculating the expected reflection coefficients. The radiation term is neglected, the

Equivalent Circuit



C_f - from internal fringing field

C_o - from external fringing field

G_o - radiation conductance

Fig. 2. Equivalent circuit of open probe.

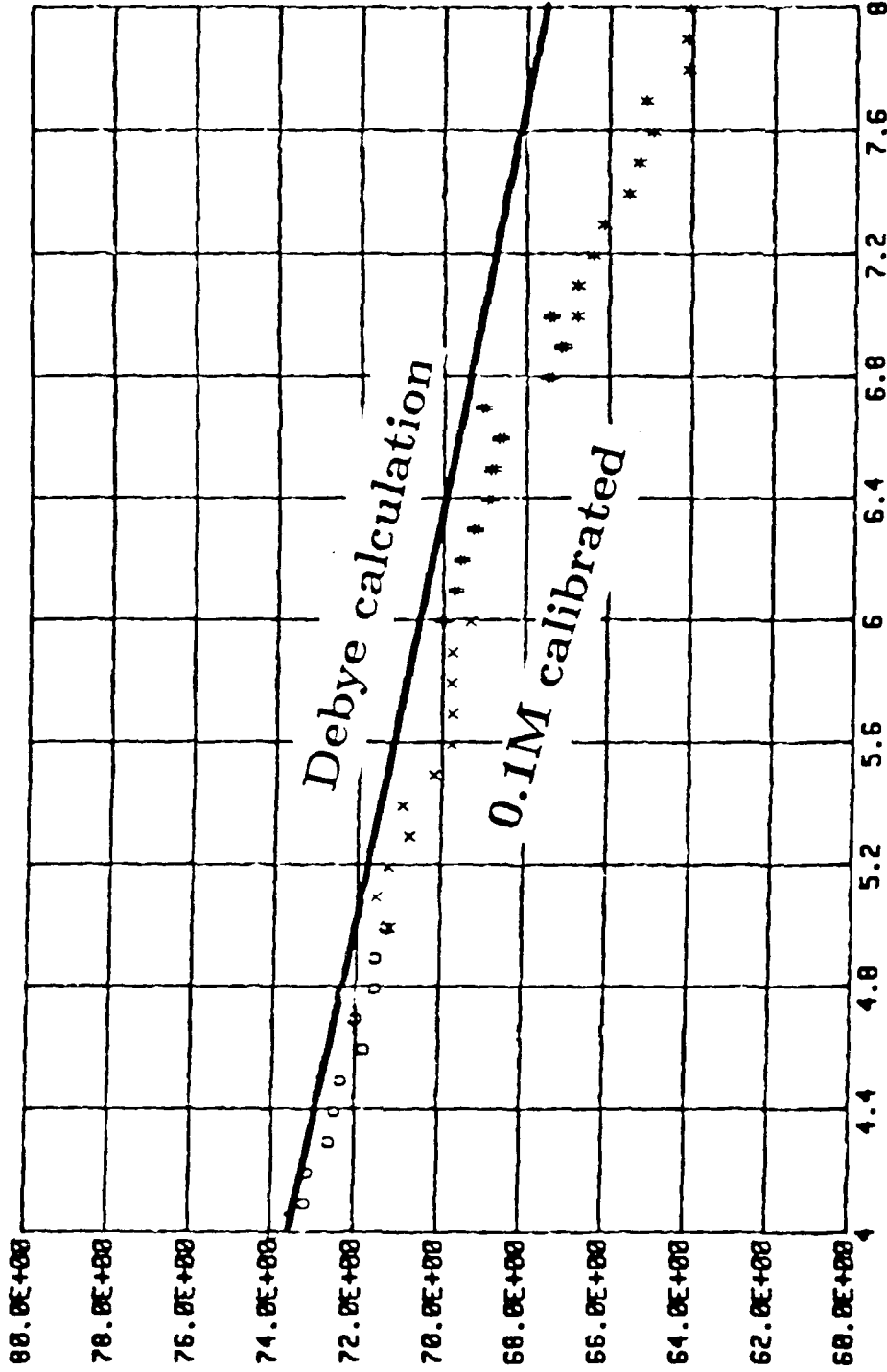
consequences of this will be discussed later. Values of C_0 and C_f can be determined by this calibration procedure [8], however, for the 3.6mm line used reliable previously determined experimental values are also available [13].

Results

To demonstrate the accuracy of the open probe technique after vector error correction is carried out at the probe tip, we made a series of measurements to test: (i) absolute accuracy in measuring one standard liquid after calibration with a different or the same standard liquid (ii) measurement repeatability in a series of measurements of the same sample and (iii) sample volume effects. Several conclusions can be drawn from these measurements: The absolute accuracy of the open probe technique is greatest when the material being measured is close in dielectric properties (both real and imaginary) to the liquid used during calibration. Because the radiation error is neglected in determining calibration impedances, the parameters of the error network are also systematically in error. However, to first order, when measurements of a similar substance to the calibration liquid are made these error effects cancel out. The absolute accuracy deteriorates as the frequency increases. Both these features are illustrated in Fig. (3) which shows the real part of the dielectric constant of 0.1M saline, measured after calibration with 0.1M saline and compared with the values calculated from the Debye equation. The absolute accuracy is better than 0.5% at 4GHz deteriorating to 5% at 8GHz. For 0.2M saline measured after calibration with 0.1M the absolute accuracy decreases from 0.6% at 4GHz to 6% at 8GHz as shown in Fig.(4).

As a measure of accuracy, the absorption coefficient calculated from Eq. (3) is a more sensitive measure than either ϵ' or ϵ'' . Fig. (5) shows the absorption-coefficient of 0.1M saline measured using two different sample volumes. Calibration was made using 0.1M saline. This figure is a worst case example of deterioration of absolute accuracy because the frequency range, 8-12 GHz, is the highest we have used to date with the open probe. However, even though the measurement error ranges from 19% to 24%, the data trend is indicated correctly and the random scatter in the data is <4%, even at 12GHz. One thing the open probe technique does not do, in the manner we have implemented it, is to introduce any structural artifacts into the measurement. Fig. (5) also shows that very little additional error is introduced even when the sample volume is decreased to 60 μ l. This is important to note when measurements must be made on expensive samples that cannot be obtained in large quantities.

0.1M measured



Frequency (GHz)

Fig. 3. Measurement of ϵ' of 0.1M saline after calibration with 0.1M saline, compared with the theoretical prediction from the Debye equation. The small discontinuities in the data at 5.6 and 7 GHz result from separate calibrations over the corresponding frequency ranges.

0.2M measured

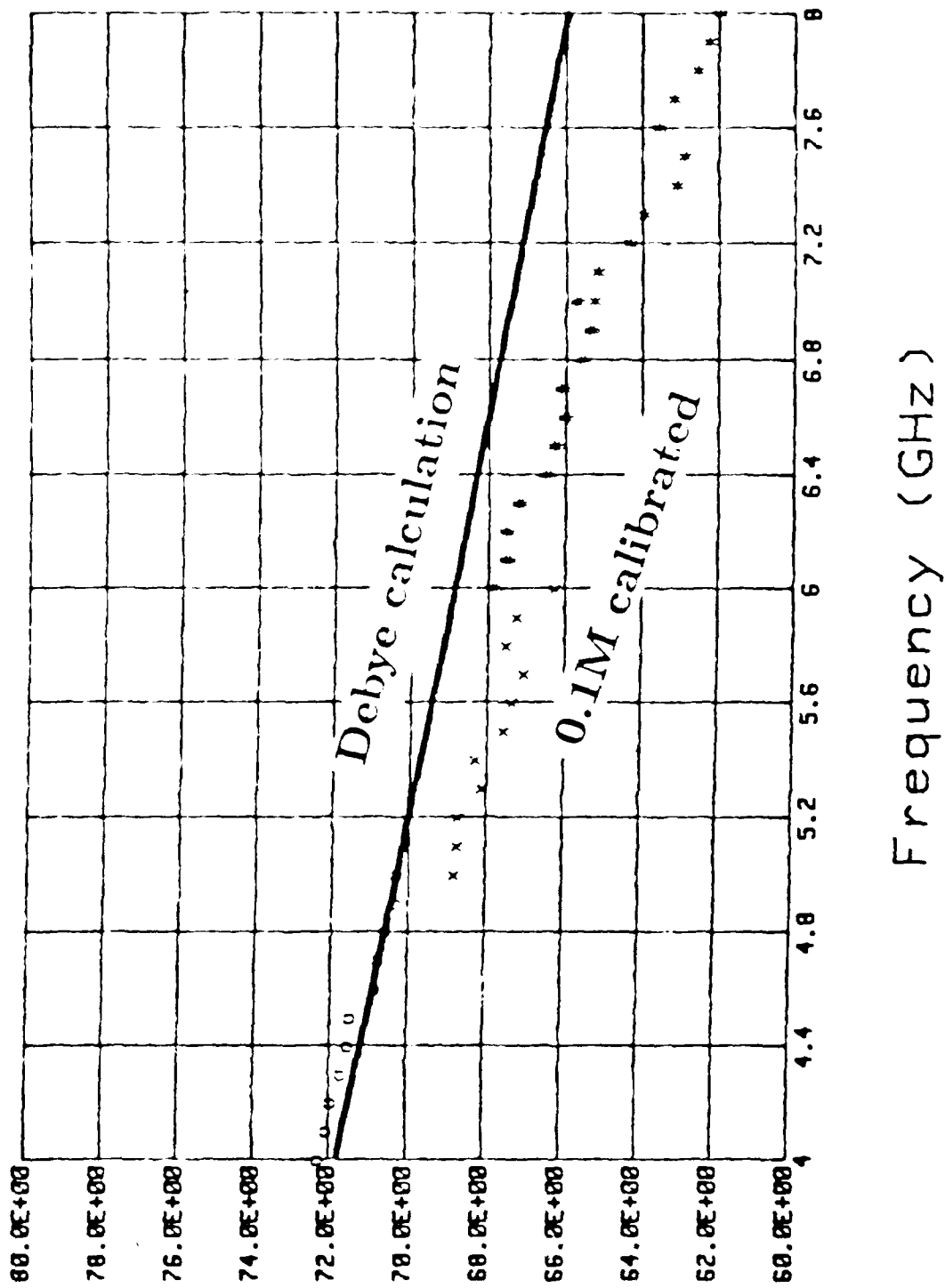


Fig. 4. Measurement of ϵ' of 0.2M saline after calibration with 0.1M saline, compared with the theoretical prediction from the Debye equation.

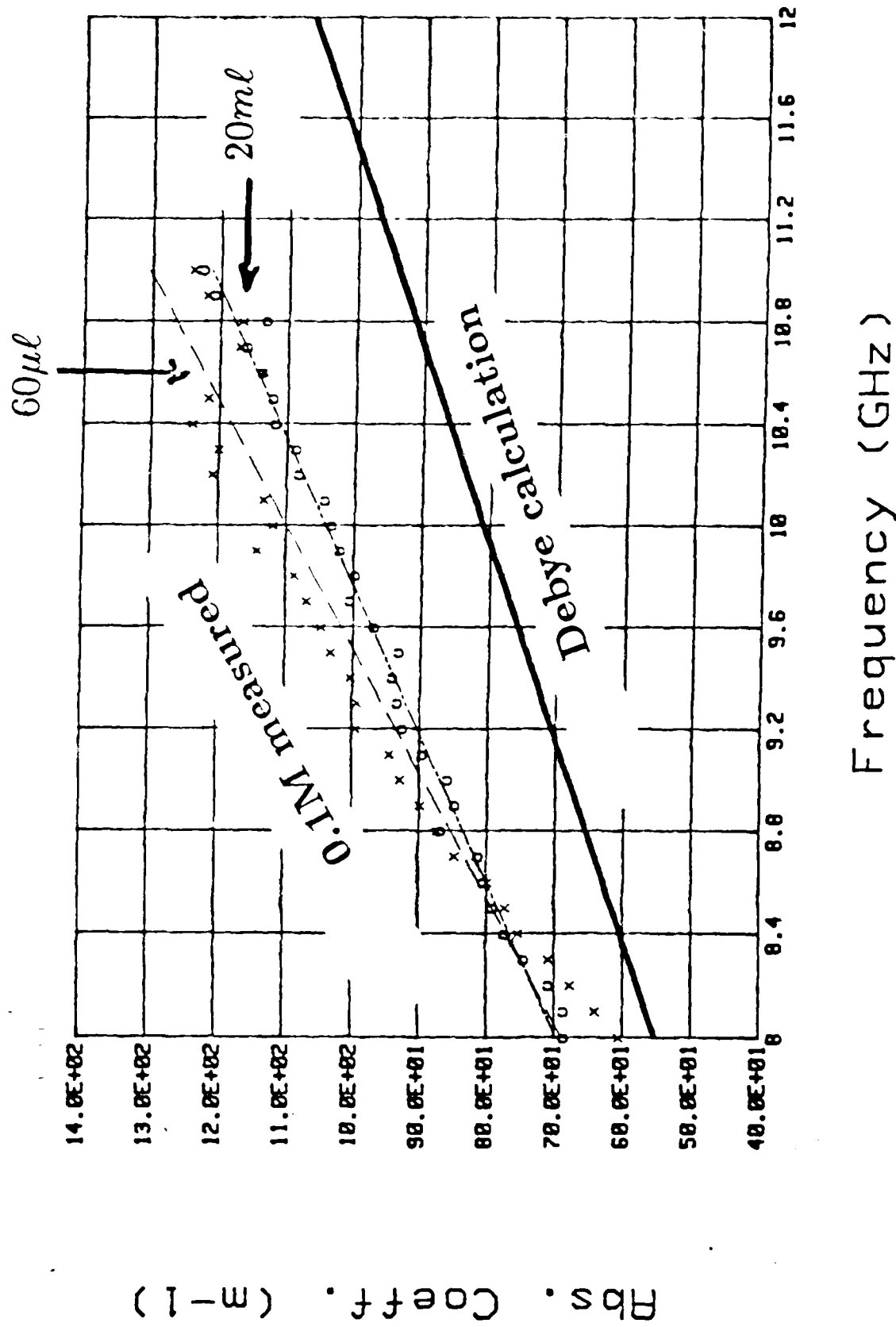


Fig. 5. The plane-wave absorption coefficient of 0.1M saline measured using two different sample volumes after calibration with 0.1M saline. The theoretical prediction from the Debye equation is also shown.

Figs. (6),(7) and (8) will serve to demonstrate the errors that can be introduced when the measured material differs from the calibration liquid. These figures shows measurements of the real and imaginary parts of the dielectric constant, and the absorption coefficient, of 0.6M saline following calibration with 0.1M in the frequency range 6-7 GHz. In Fig.(7) the error in ϵ'' is 11%, but with less than 3% random scatter. The error in ϵ' shown in Fig.(6) is much smaller: this behavior is typical. The error in ϵ' in the same range is only 3%. Multiple measurements of the same sample are repeatable within better than 3%.

In conclusion, we have shown that the open-probe technique is flexible, repeatable, can be used with small quantities of sample, and is accurate at frequencies where the probe diameter is significantly less than the wavelength in the sample. Even at higher frequencies the behavior of the probe, although monotonically slightly inaccurate, still allows accurate comparison of one material with another, is repeatable, and does not introduce artifactual features into data.

0.6M measured

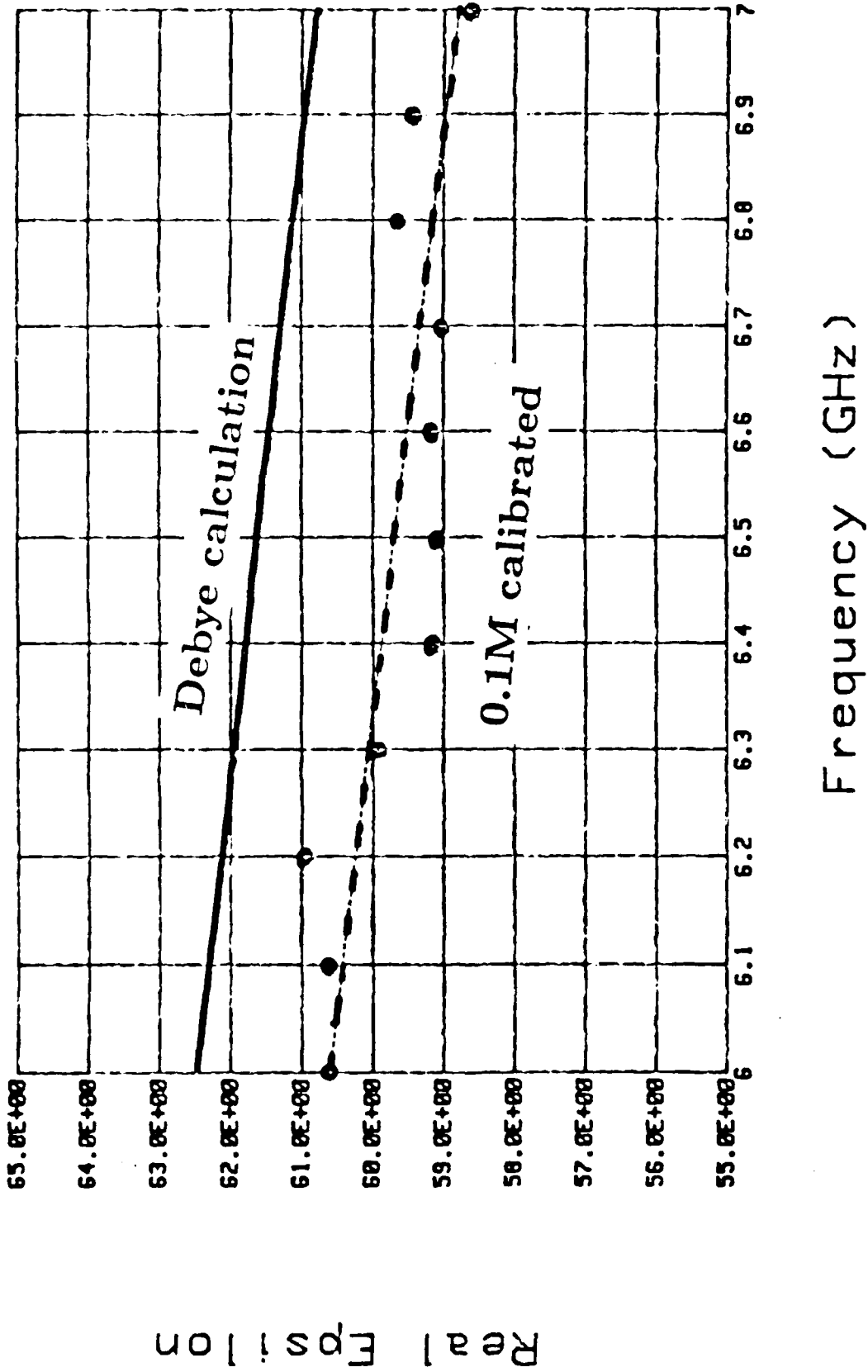
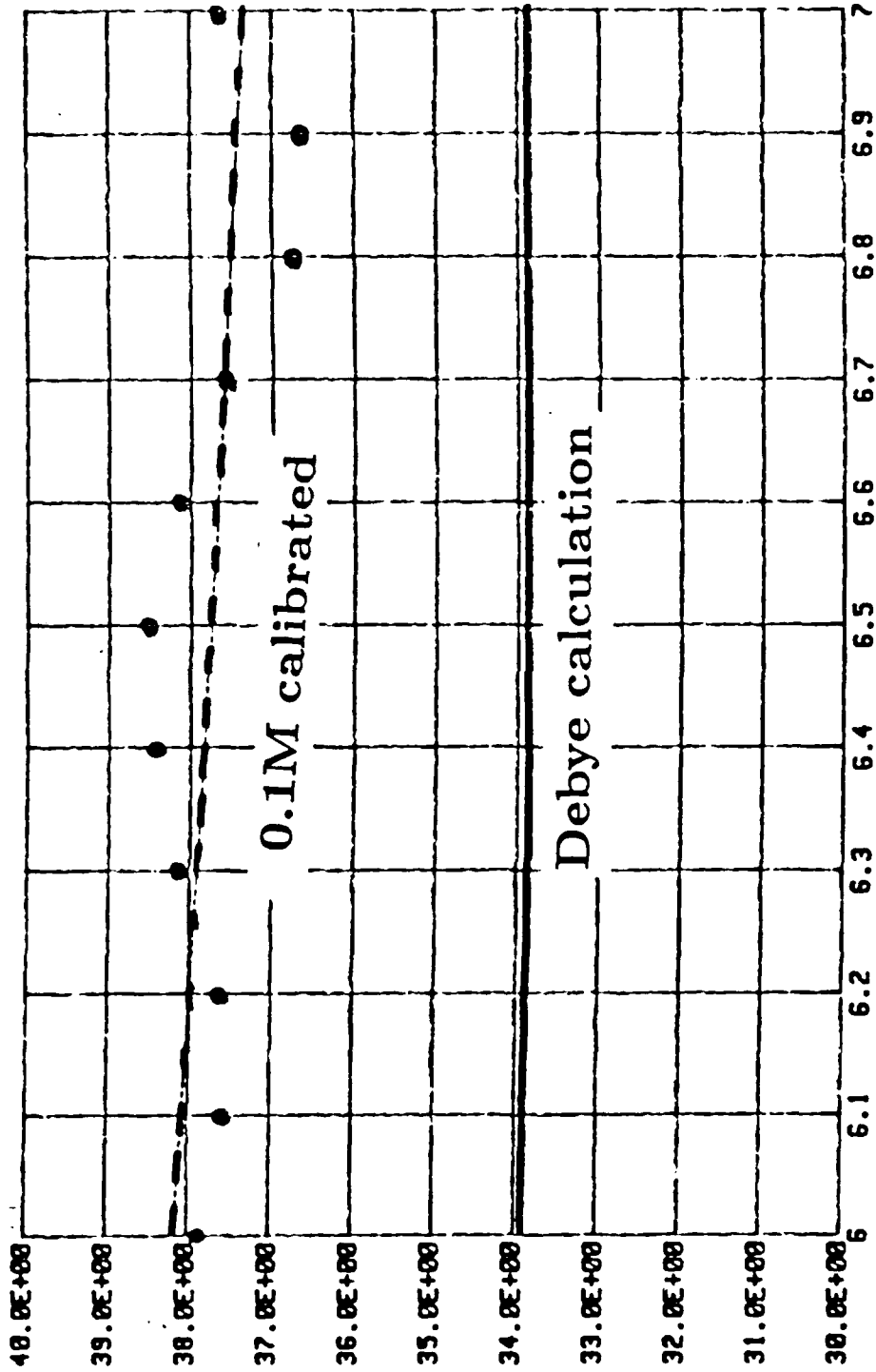


Fig. 6. Measurement of ϵ' of 0.6M saline after calibration with 0.1M saline, compared with the theoretical prediction from the Debye equation.

0.6M measured



Frequency (GHz)

Fig. 7. Measurement of ϵ'' of 0.6M saline after calibration with 0.1M saline, compared with the theoretical prediction from the Debye equation.

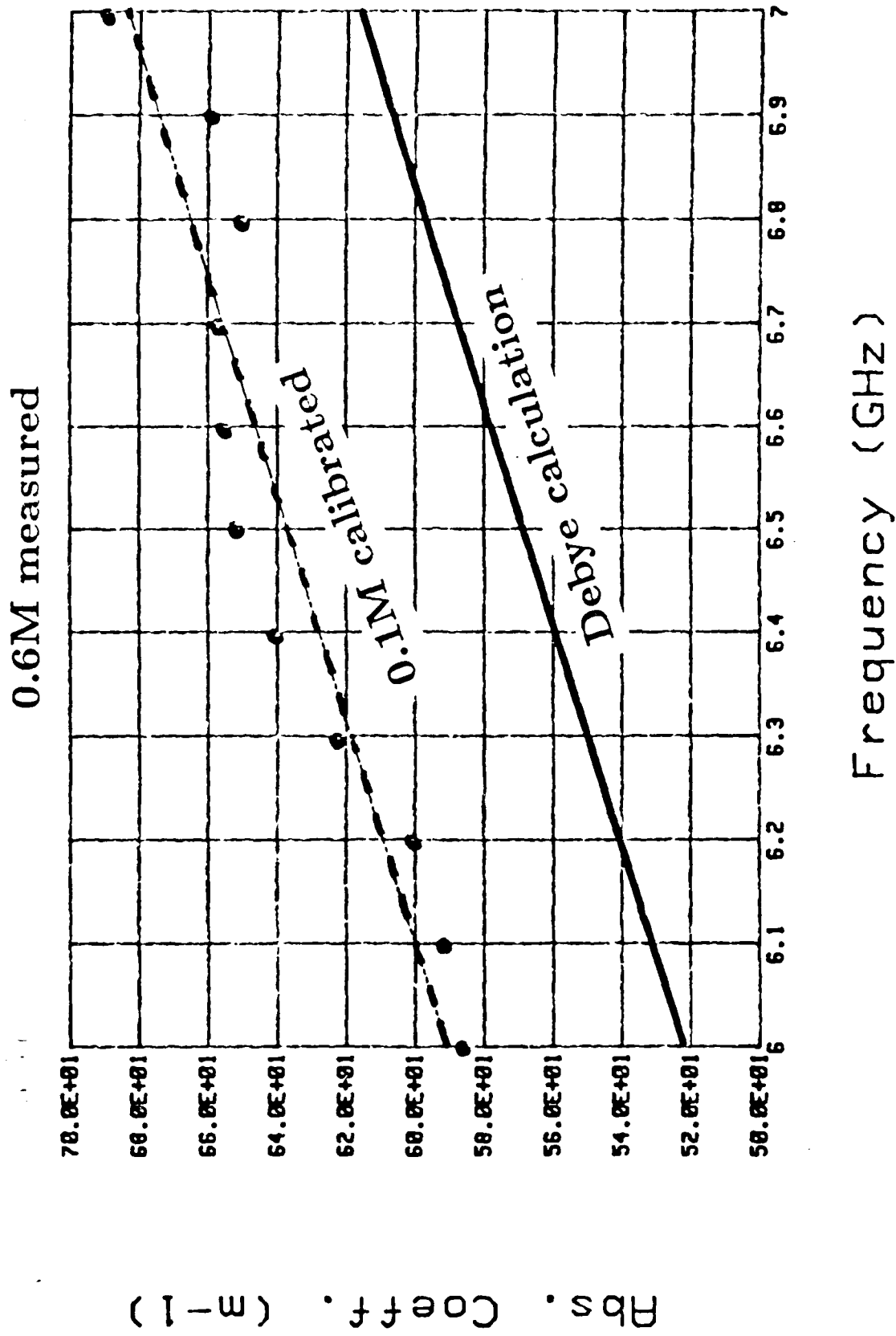
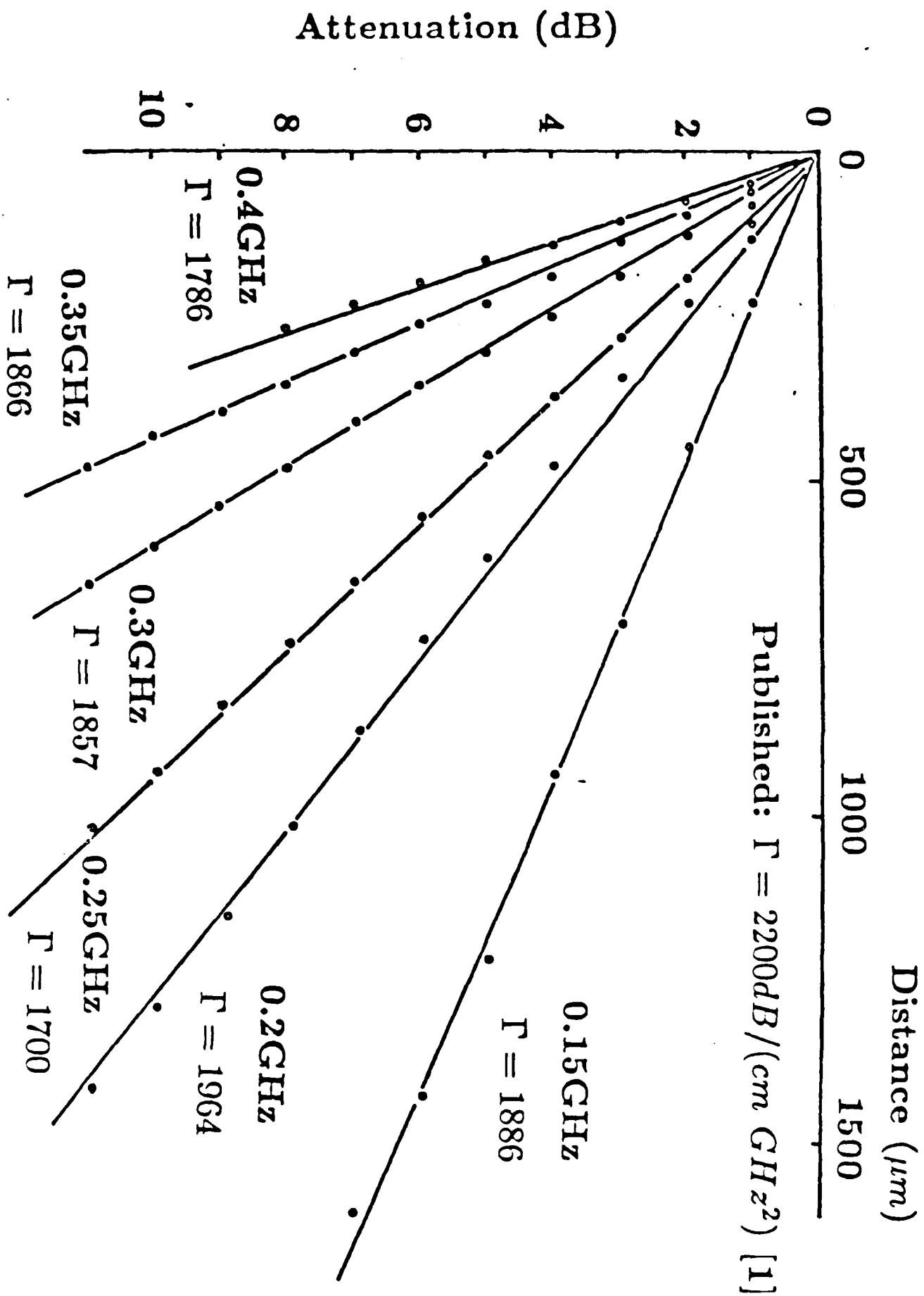


Fig. 8. Measurement of the absorption coefficient of 0.6M saline after calibration with 0.1M saline, compared with the theoretical prediction from the Debye equation.

Fig. 19. Measured acoustic attenuation of standard 0.86% saline buffer containing Tris.



MICROWAVE DETECTION

A series of experiments was begun to explore the possibility that a DNA solution might emit microwave radiation when acoustically excited. It was expected that a pure water sample would yield no signal, while a DNA solution might yield a small signal due to the presence of DNA, and that this signal might exhibit a resonance based on the length of the DNA molecule. The experiment yielded an unexpected result: pure water produced a clear signal, while the DNA solution produced a slightly smaller signal. Then a more careful series of experiments was performed to understand these results.

Frequency Domain: The first experiment was performed using an acoustic transducer excited by a CW RF signal, coupling the sound wave into a solution located between the cell and a nearby antenna: see Fig. (20). The cell substrate was made of $LiNbO_3$, an inert single crystal material which exhibits piezoelectricity, pyroelectricity, and just about every other possible interaction. The antenna was fed into a high gain RF amplifier and then to a spectrum analyzer. The detected signal was taken versus frequency for several different solutions between cell and antenna, and it proved very difficult to distinguish between different solutions using this method. One reason is that it is impossible to differentiate between RF signals not of interest arising from such sources as feedthrough. Thus, a second experiment was attempted with time resolution, to sort out the various contributions according to their timing.

Time Domain: To add time resolution to the experiment, the incoming RF signal was pulsed using a SPDT microwave switch. The pulser used to drive the switch also provided a triggering signal used to synchronize a sampling oscilloscope to the amplified detector output. This arrangement is shown in Fig. (21). RF pulses were observed at the detector, with timing as shown in Fig. (22). The pulses are shown as negative pulses because the detector had negative polarity.

The first and largest pulse is composed of RF feedthrough from two sources: the RF pulse applied to the cell transducer, and RF components of the switching pulse applied to the switch. The latter switching noise causes the small parasitic lobe on the main feedthrough pulse. A second feedthrough pulse is observed at a later time, corresponding to one round trip acoustic transit time through the cell substrate. This is when the acoustic pulse returns to the transducer after its round trip and is reconverted to an RF pulse.

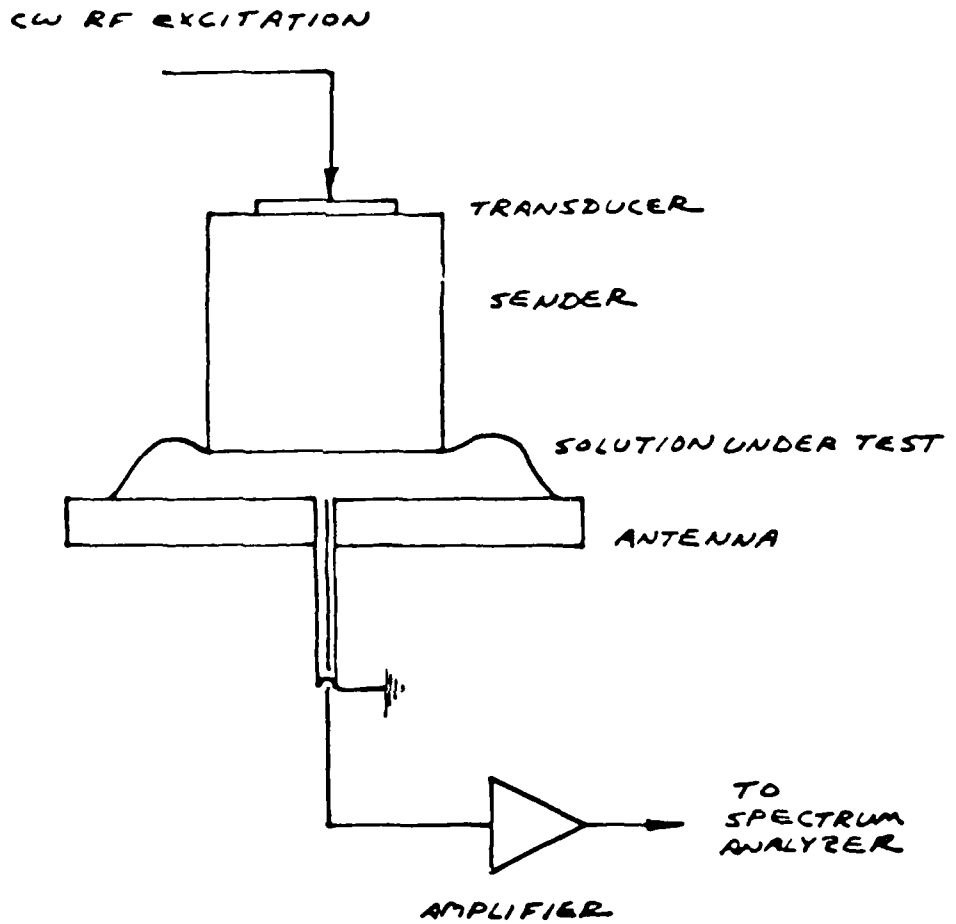


Fig. 20. Apparatus for non-time-resolved detection of acoustically generated microwaves.

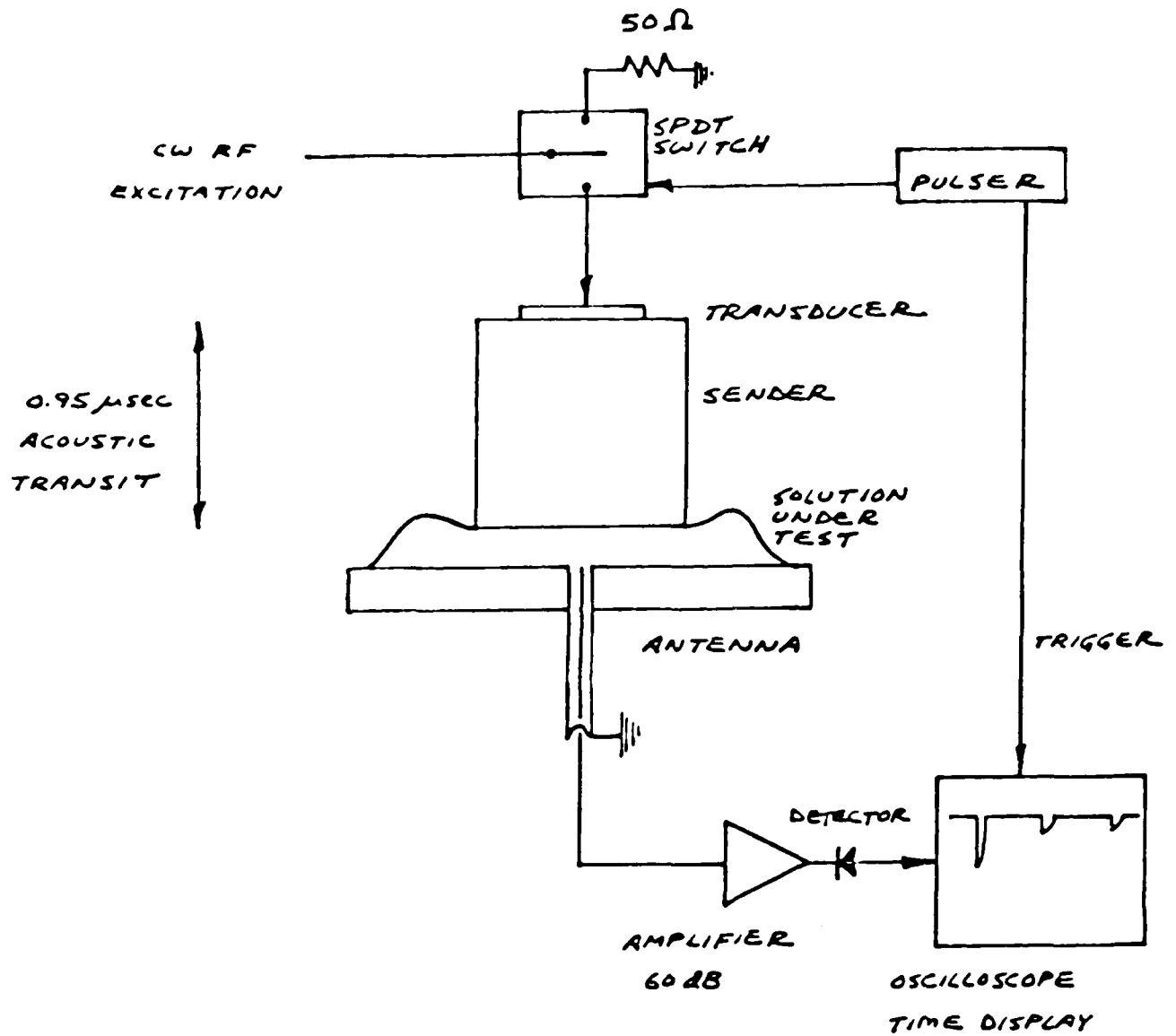


Fig. 21. Apparatus for time-resolved detection of acoustically generated microwaves.

Fig. 22a Time sequence of microwave pulses detected by antenna.

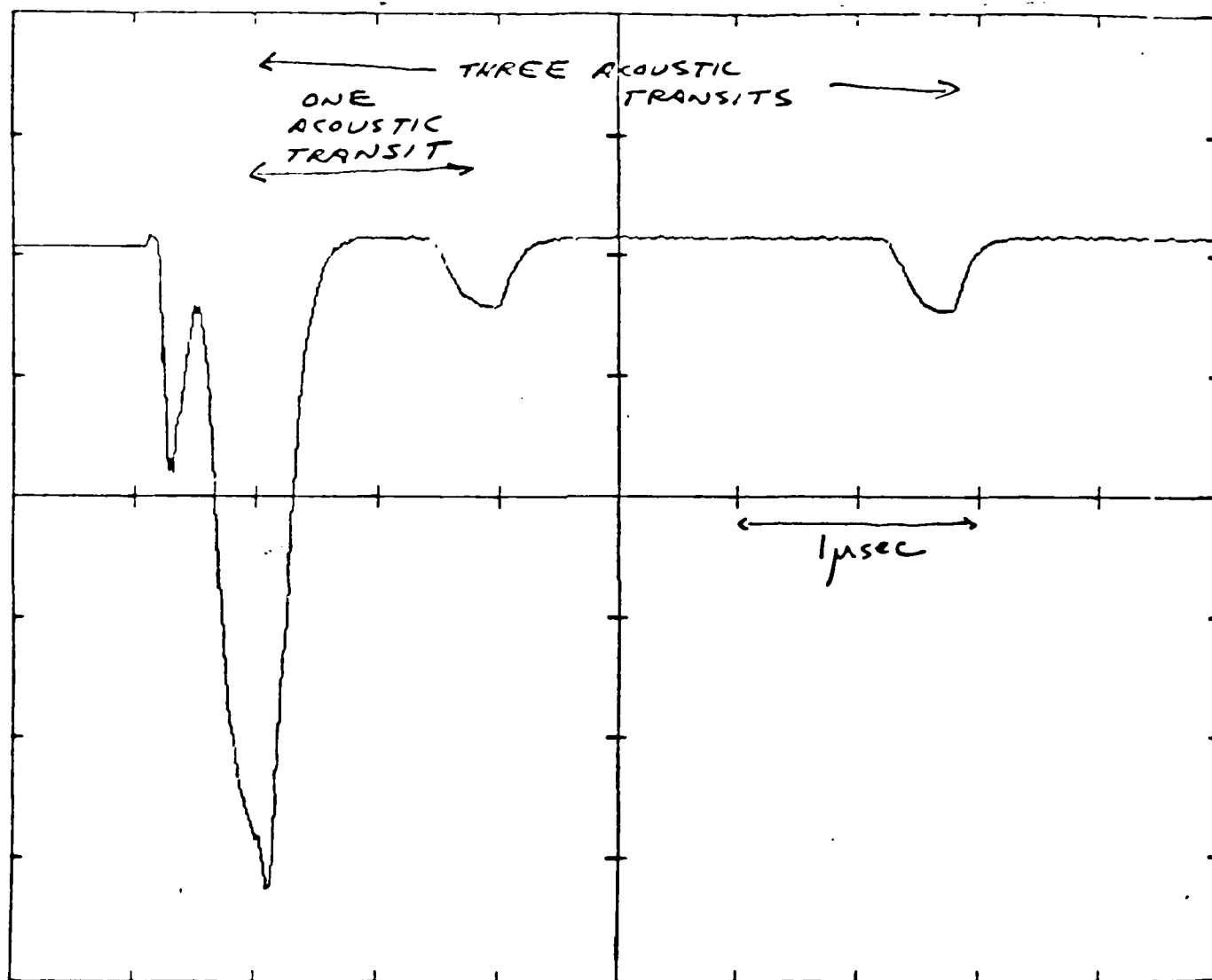
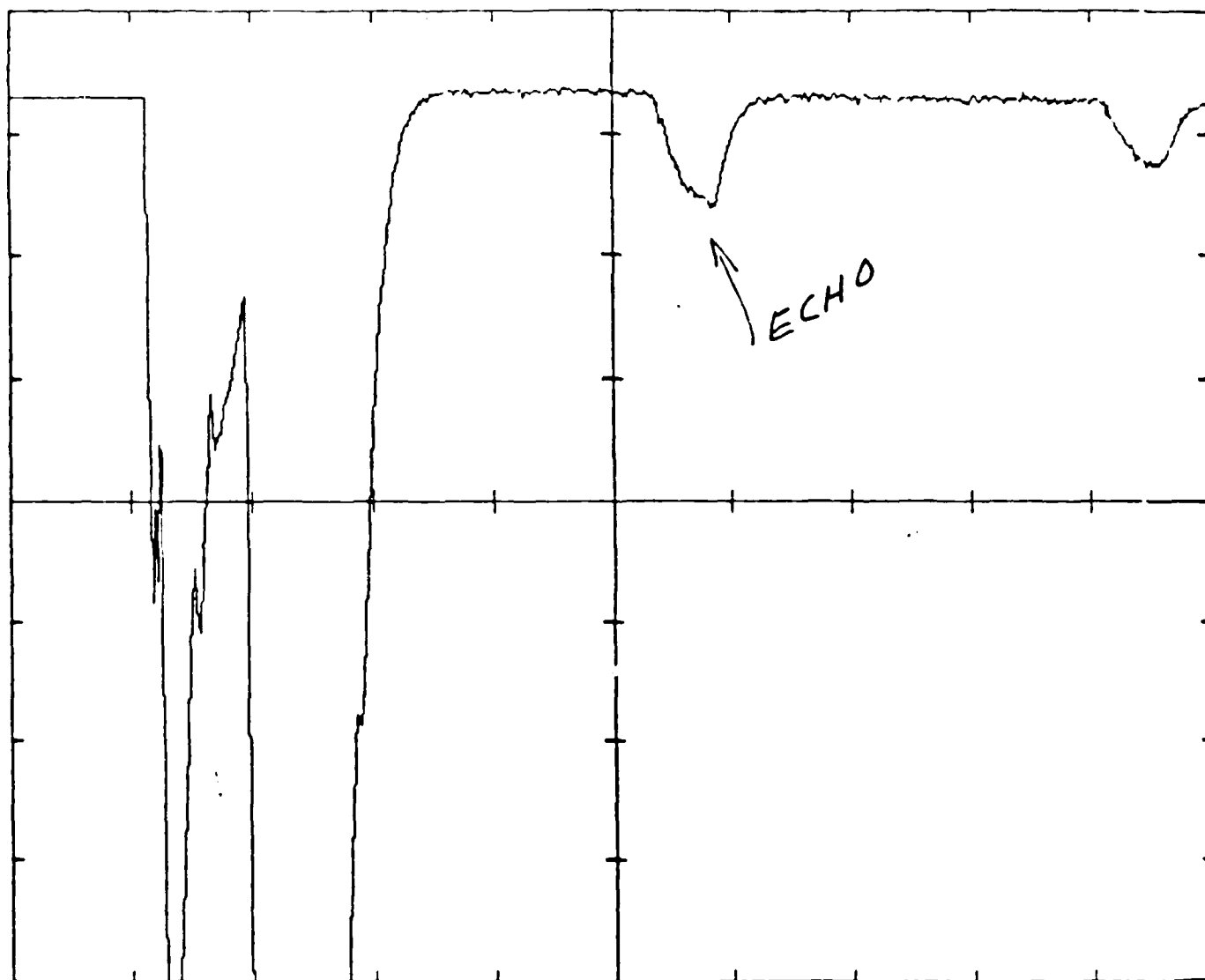


Fig. 22b Further detail of time sequence of microwave pulses detected by antenna.



Between those two feedthrough pulses, an unexpected pulse appeared, at a time corresponding to the arrival time of the acoustic pulse at the cell/solution interface. This was the pulse of interest in this series of experiments, and some effort was applied toward identifying its origin. Note that the timing of these pulses identifies them with no uncertainty. The long acoustic delays are unmistakable and correspond precisely to the length of the cell substrate.

The magnitude of the acoustically delayed microwave pulse was measured versus frequency for both pure water and DNA solutions. The response was measurably weaker with the DNA solution, and this difference was repeatable: see Fig.(23). Thus this pulse permitted different solutions to be distinguished, a property of interest for probing such solutions. Note that the sharp frequency variations merely reflect the frequency response of the acoustic transducer, and have no other significance.

Several mechanisms for the generation of such an interface pulse were considered including:

- microwave response of the bulk liquid
- response of a liquid dipole layer at the interface
- an acousto-electric field generated within the substrate or at the interface
- an acoustic wave striking the antenna
- other experimental artifacts

A series of experiments was done to narrow down the possibilities.

The first procedure was undertaken to eliminate the possibility that the signal arose from an acoustic wave traveling through the liquid and striking the antenna, inducing a signal by modulating the antenna impedance or by some other effect. The antenna was moved away from the cell in measured amounts. The signal was observed to decrease in amplitude, but its time of arrival did not change at all. The antenna was moved far enough to bring about a 500 nsec acoustic delay in the solution, and no such delay was observed even though the arrangement permitted much better time resolution. Thus no acoustic transmit time across the solution layer was involved.

Next, the response was observed as a function of distance from the cell substrate to the antenna, using several liquids in between. The results appear in Fig.(24). Note that the slopes of all the lines are nearly equal: this implies that signal propagation across the liquid layer is

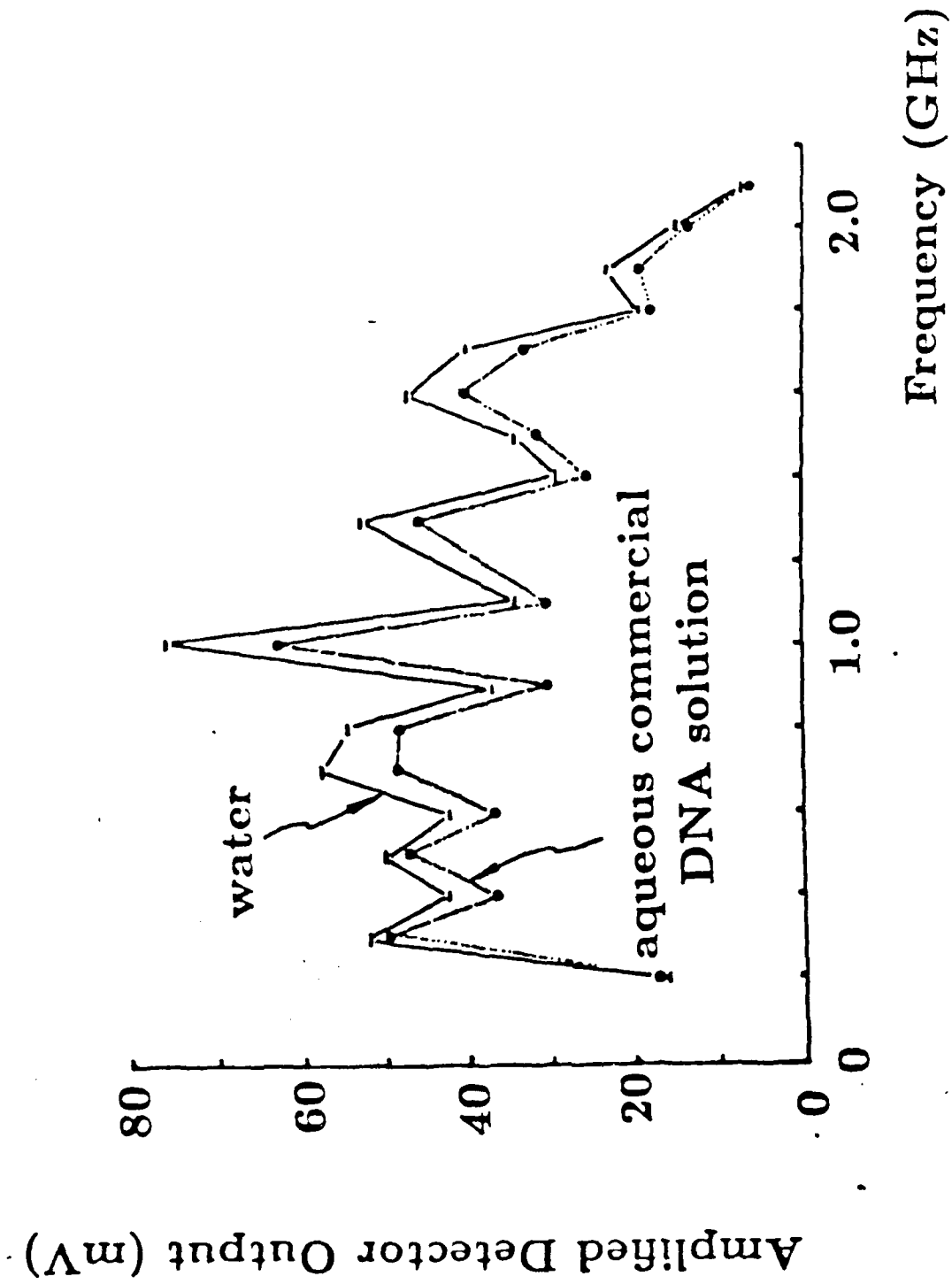
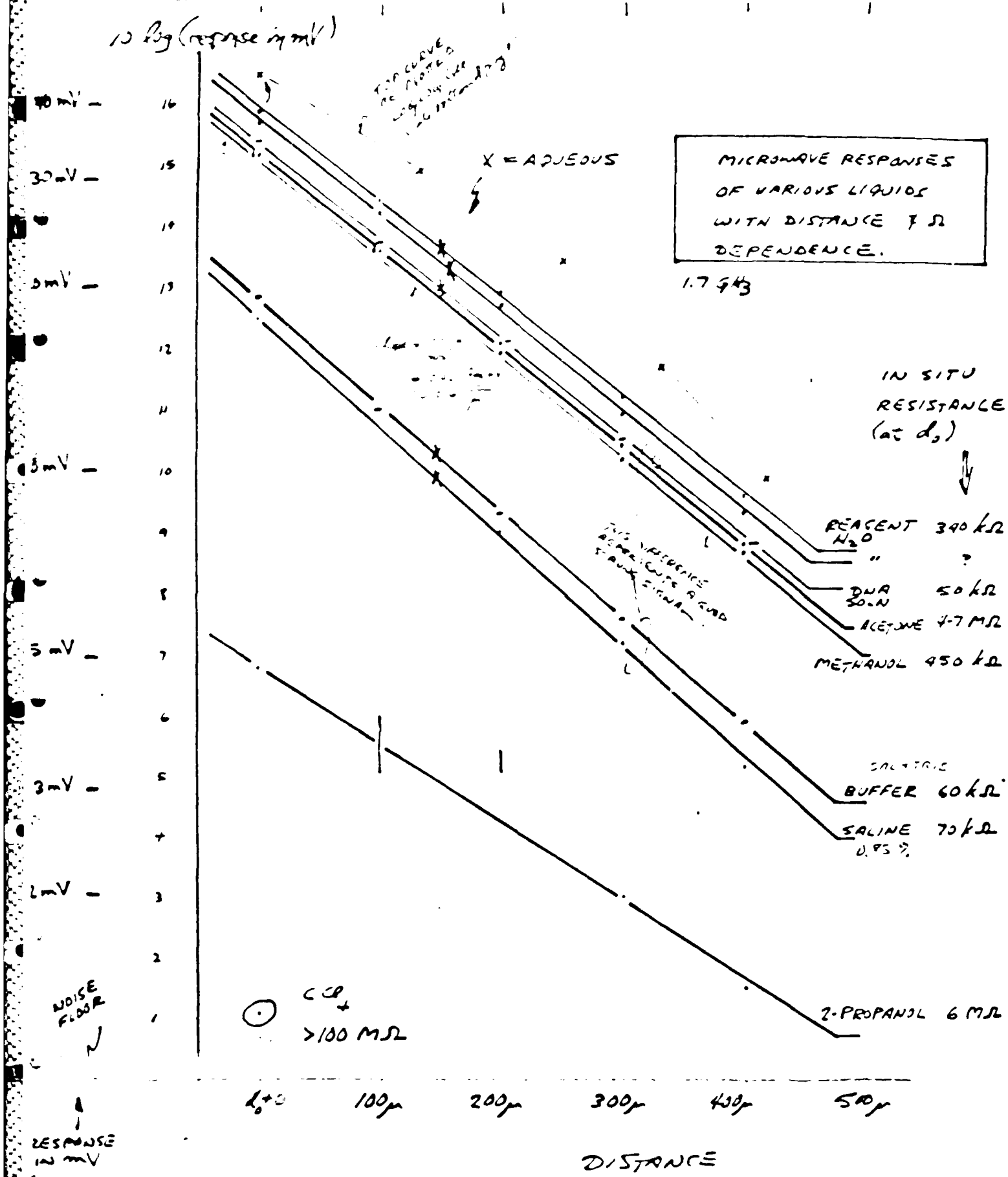


Fig. 23 Preliminary microwave detection results for water and aqueous solution of commercial DNA.

Fig. 24. Microwave signals obtained using different liquids between transducer and antenna. Parametric dependence on factors such as distance to the antenna and liquid impedance are shown.



independent of the specific liquid there, although the magnitude of the response at any fixed distance does depend on the liquid. This implies that the signal originates from the interface and not from the bulk liquid.

To quantitatively investigate the dependence of signal strength on the liquid properties, a series of saline solutions of various salinities was prepared. Response was then observed at a fixed distance from substrate to antenna for each solution, with an observation using pure water following each one using a saline solution. The response versus salinity was compared to two parameters of the liquid dependent on salinity: conductivity and dielectric constant. The results appear in Fig.(25). Note that the response closely tracks the dielectric constant of the solutions, while its behavior is not at all like the conductivity: as conductivity rises, the response falls. This eliminates the possibility that the signal arises from conductive coupling between any fields generated at the interface and the antenna.

The data of Fig.(24) was also rearranged to show response as a function of dielectric constant, and the results appear in Fig.(26). While the graph does not show nearly the clean correspondence between response and dielectric constant as is seen in Fig.(25), a trend toward increasing response with increasing dielectric constant appears. For the purpose of producing these curves literature values of the dc dielectric constant for the liquids were used.

These results support the conclusion that the signal arises from fields existing within the cell substrate which are capacitively coupled to the antenna; the capacitance is a function of the intervening liquid dielectric constant, causing the response to track the dielectric constant.

It is reasonable to suppose that the $LiNbO_3$ substrate generates internal electric fields due to the passage of the acoustic wave (these are called parasitic fields, due to the piezoelectricity of the substrate) and that these fields are sensed by the antenna in close proximity. The strength of the signal is mediated by the dielectric constant of the liquid between substrate and antenna, which determines the coupling capacitance.

Microwave Detection with a Thick Slab

In an effort to further quantify this supposition, an attempt was made to measure the response as a function of substrate material and orientation. This is a difficult measurement to make without simply manufacturing numerous acoustic transducers on various substrates, and

Fig. 25a Acoustic → microwave response for saline solutions.

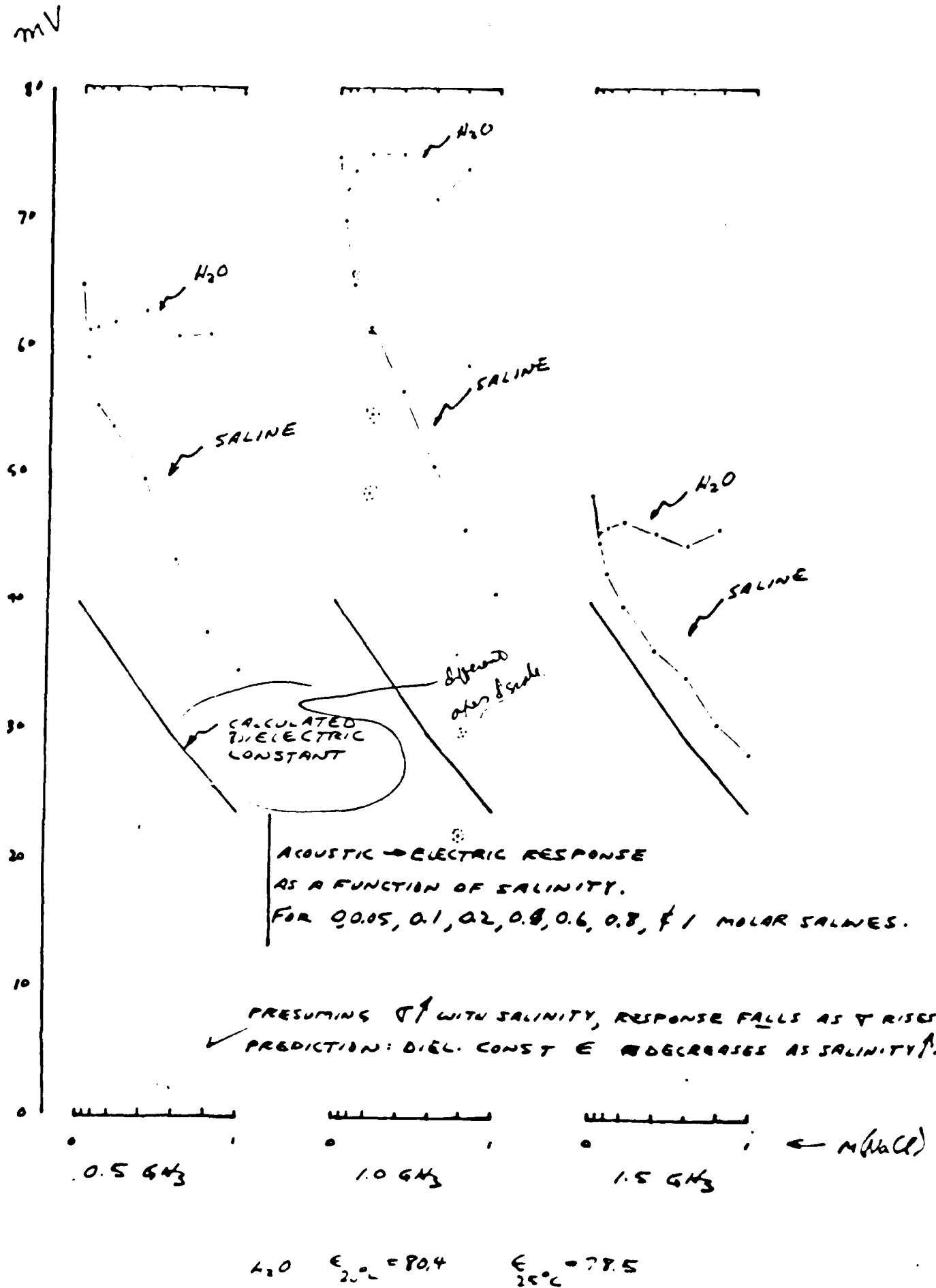
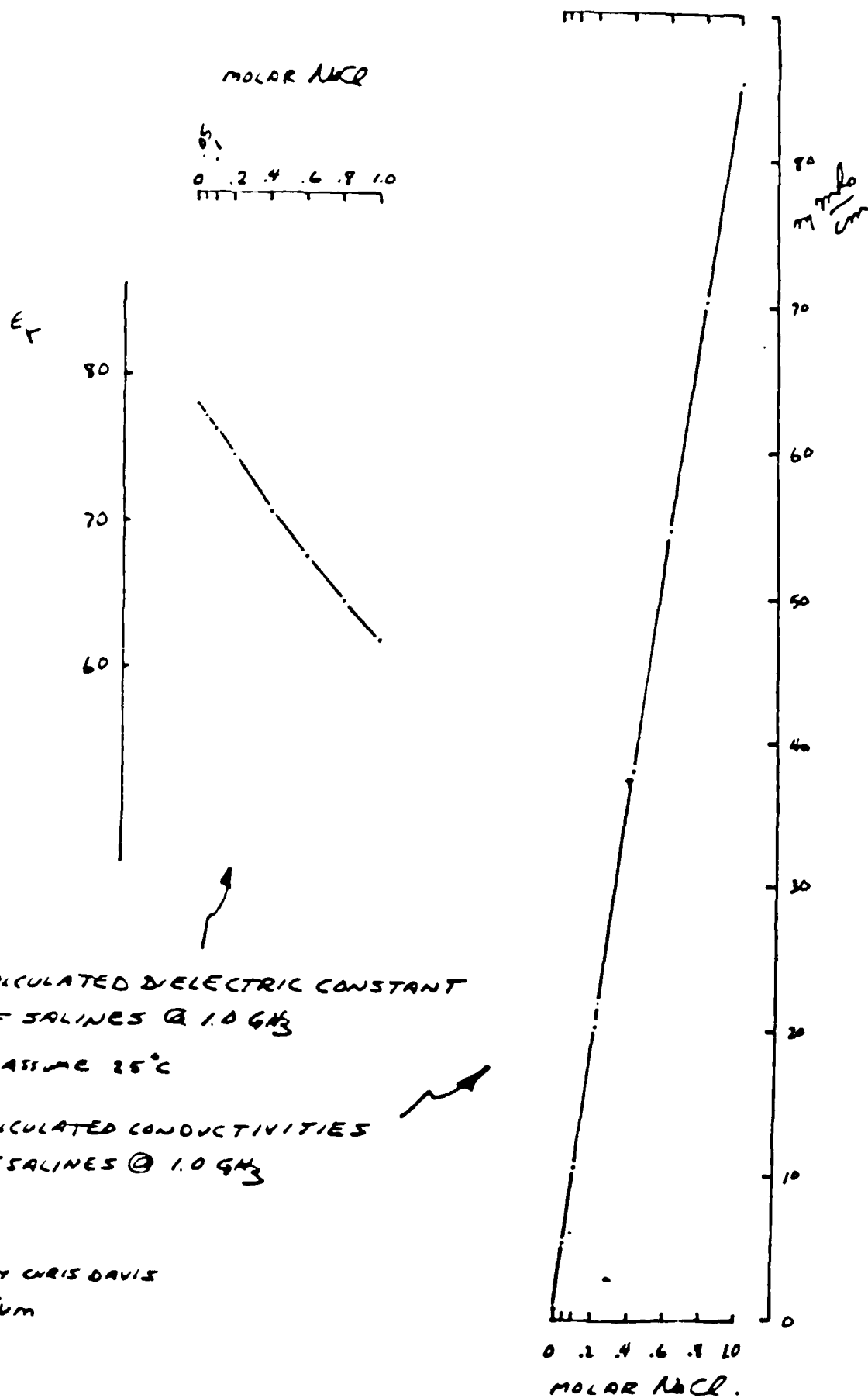


Fig. 25b. further detail of parametric dependence of acoustic \rightarrow microwave response of saline solutions.



CALCULATION BY CHRIS DAVIS
 NP-1000 RTEG/UM
 30 AUG 85

10 log [response in mV]

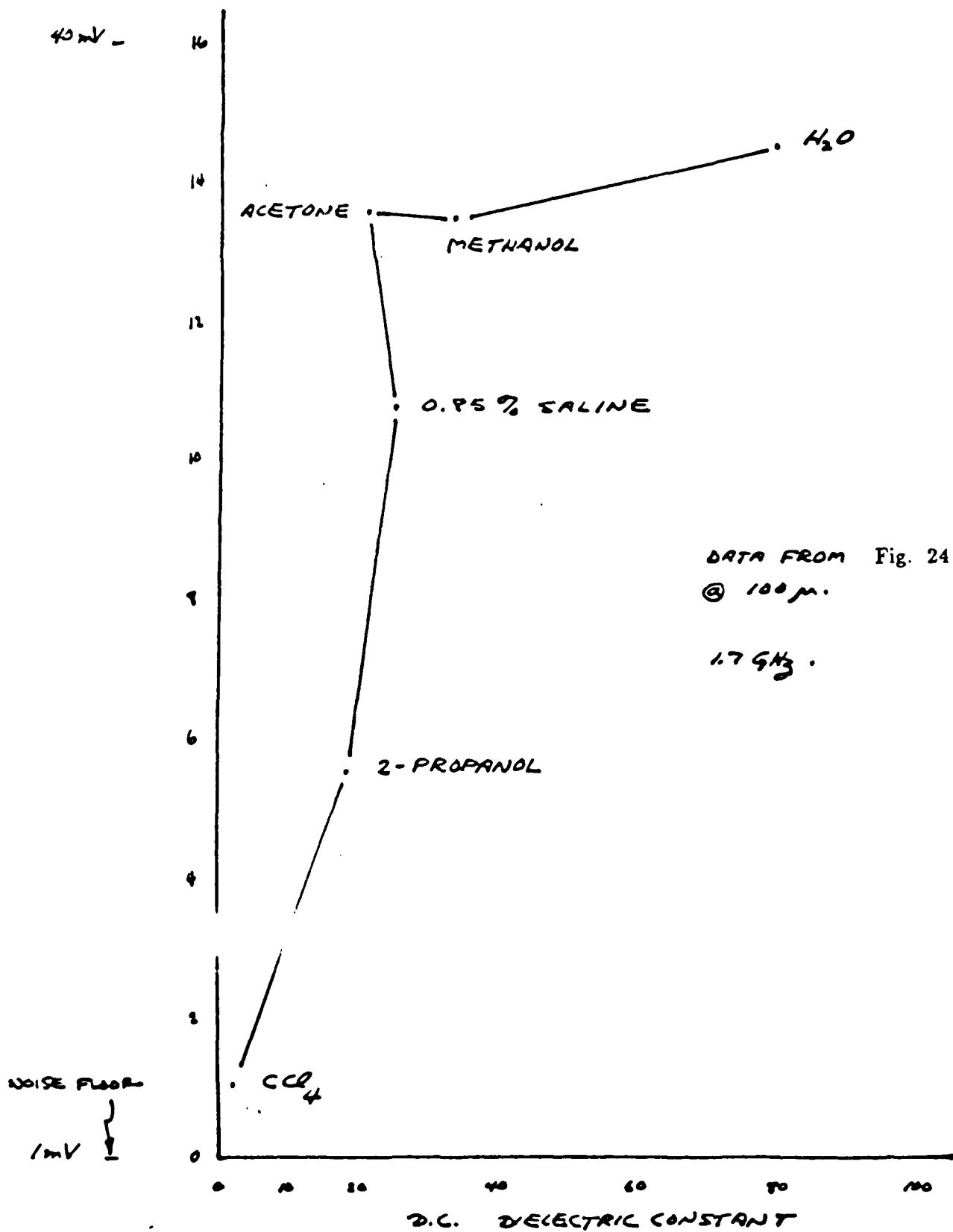


Fig. 26. Acoustic → microwave response versus dielectric constant for several liquids.

this was not an option. Instead, an additional "thick slab" of material was inserted between the cell substrate and the liquid solution, as shown in Fig.(27). The acoustic wave was passed from the substrate to the thick slab via a very thin layer of water, which is the liquid with the lowest acoustic attenuation available. The slab had to be sufficiently thick to be able to observe the acoustic reflection from the slab/liquid interface; this permitted measurement of the strength of the acoustic pulse arriving at that interface, a quantity necessary to obtain quantitative results.

A variety of thick slabs was available for use, made of $LiNbO_3$ and of fused quartz. Three propagation directions were available in $LiNbO_3$, while the quartz substrates were isotropic. The slabs had to satisfy certain thickness criteria with relation to the cell substrate so that the reflection from the slab/liquid interface could be observed without interference from some other pulse echo, for example the double round trip transit within the cell substrate. Fig.(27) includes the signal notation used below to normalize the resultant data.

The acoustic transducers had been fabricated in two different batches. The first batch had an acoustic transit time which did not permit the resolution of the acoustic pulse returning from the liquid interface; this pulse was masked by other pulse echos. However, the substrates of the second batch of devices did permit that resolution, and these experiments began as soon as a device from the second batch was available.

To obtain quantitative measurements of the response for the various substrate materials and orientations, the size of the pulse reaching the slab/liquid interface had to be inferred. This required the measurement of the sizes of the pulses at two points in the RF system: the pulse reflected from the slab/liquid interface, and the pulse received from the antenna. Thus two pulses were monitored as different slabs were switched in and out of the apparatus.

With reference to Fig.(27). The input RF pulse, S_{in} , is assumed to have some fixed power A_0 . It then undergoes several transmittances: T_1 at the cell transducer, T_2 in the cell substrate, T_3 at the cell/slab interface, T_4 in the thick slab, and a reflection R_5 at the slab/liquid interface. The microwave signal which is observed by the antenna is related to the acoustic pulse by T_6 , which includes the acoustic-to-electric conversion that occurs near the interface. T_6 is the quantity of interest.

The pulse reflected from the slab/liquid interface undergoes the same set of transmittances

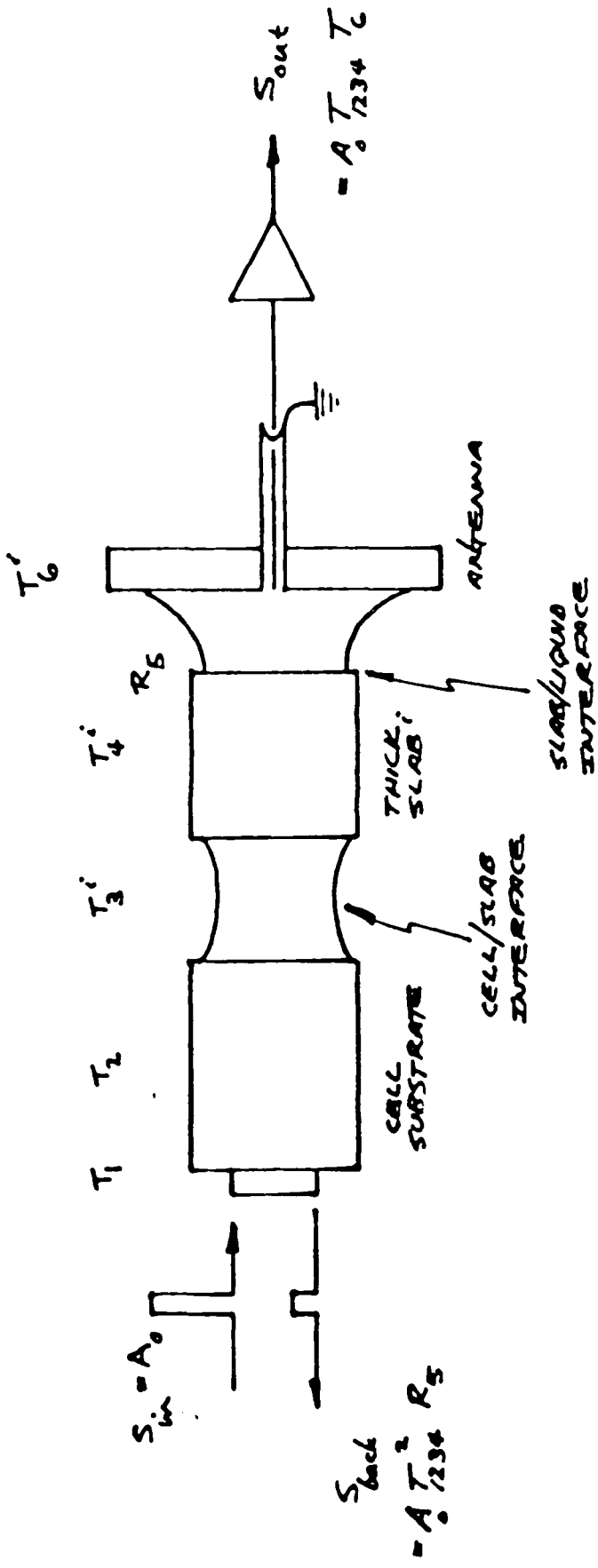


Fig. 27 Thick slab experiment used to resolve origin of microwave signals, showing geometry and notation.

Assume: A_0 FIXED.
 R_5 FIXED.
 T_2 FIXED.
 T_3 & T_6 DEPEND ON SLAB i .

NOTE: T_6 & R_6 ARE NOT SIMPLY RELATED.
 R_6 IS SIMPLE ACOUSTIC REFLECTION.
 T_6 ENCOMPASSES ACOUSTIC \rightarrow ELECTRIC CONVERSION.

again, emerging from the transducer as an "echo" with power:

$$S_{\text{back}} = A_0 T_{1234}^2 R_5$$

The detected signal has power:

$$S_{\text{out}} = A_0 T_{1234} T_6$$

Now suppose that the "out" and "back" signals are measured for one slab, and a new slab is then inserted. A new set of signals is generated:

$$S'_{\text{back}} = A_0 T_{12}^2 T'_{34} R_5; \quad ; \quad S'_{\text{out}} = A_0 T_{12} T'_{34} T'_6$$

where the primes indicate that the new slab changes the transmittance values.

A little algebra yields an expression for the relative value of T_6 in terms of the "out" and "back" signals:

$$\frac{T'_6}{T_6} = \frac{S'_{\text{out}}}{S_{\text{out}}} \sqrt{\frac{S_{\text{back}}}{S'_{\text{back}}}}$$

Or in decibels:

$$\Delta T_6 = \Delta S_{\text{out}} - 1/2 \Delta S_{\text{back}}$$

This is the basis of the normalization applied to the data taken using the various thick slabs.

The experiment was carried out by fixing the thick slab to the antenna and then positioning the assembly as a unit beneath the cell substrate. A drop of water provided coupling between cell and slab (vacuum grease did not conduct the acoustic wave). It proved difficult to position the cell and slab for maximum coupling between them: the thin water layer acted as a resonator and had to be carefully tuned to optimize acoustic transmission. Yet this could be done, and good coupling could be obtained.

To compare the measured results to a theoretical model, the parasitic fields associated with acoustic waves proceeding in different directions in $LiNbO_3$ were estimated by appropriately rotating the piezoelectric tensor, which gives an electric field arising from a strain field. In quartz, this effect is expected to vanish since materials with inversion symmetry are not piezoelectric.

CELL SHAPE DEFORMATIONS IN STRONG ELECTRIC FIELDS

The alignment of cells in strong electric fields is a well known phenomenon, as is their controlled rotation in appropriate time-varying fields. However, theory predicts that a cell will deform in an electric field. For example a spherical cell will become prolate along the direction of the applied field. This effect is not a large one and cell shape deformations from spherical to a few percent ellipticity should require fields on the order of 100kV/m. To attempt to observe this effect we constructed the apparatus shown in Fig.(28). Cells are placed in solution in an arrangement in which light scattered from a laser beam passing through the medium can be observed transverse to both electric field and laser beam. The samples are contained in a standard 10mm \times 10mm optical cuvette into which two tantalum electrodes are immersed. The scattering cross-section of the suspended cells depends on their shape and orientation. We used modulated fields at frequencies up to 1kHz and looked for synchronous changes in scattered intensity. We had estimated that changes in cross-section of on the order of 1% should occur with the field strengths we could reach - up to 76kV/m. To reach fields of this magnitude we could not work with cells in conventional media as the conductivity of such media is high and shunts the applied field to a low value. We used both *E. coli* and mouse lymphoma cells in these experiments. In each case the cells were centrifuged and resuspended in 3mM sucrose solution several times until the conductivity of the solution was low enough not to load the applied field.

We did observe synchronous scattering from the suspended cells, but not on a reproducible basis. For some samples the signal at the 2nd harmonic of the applied field was larger than the fundamental. To test whether the observed signals were real, we examined the scattering from 1 μ m and 10 μ m glass microspheres suspended in solution. To our surprise we continued to see synchronous scattering, yet we did not believe that rigid glass microspheres would have deformed enough to produce any effect. We interpret these signals as arising from local vibration of the suspended particles about their equilibrium position. Such vibration could be expected for any small suspended particle with a net charge. We concluded that with the fields available to us it was not possible to prove conclusively how much of the observed signal arose from artifactual causes and how much resulted from actual shape change.

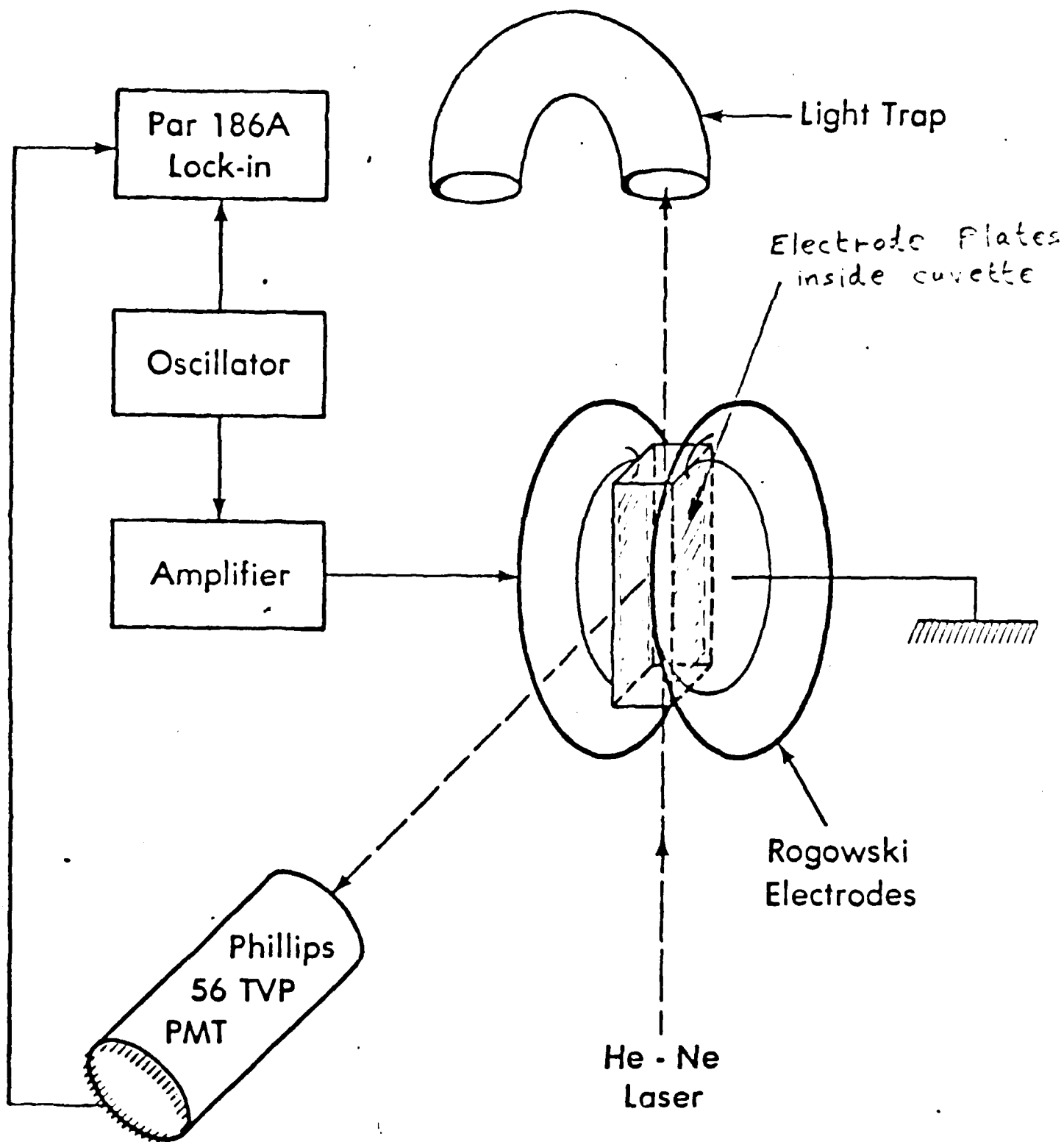


Fig. 28. Apparatus used to search for electric-field-induced cell shape change by observing synchronous changes in light scattering.

REFERENCES

- [1]. Swicord, M. L. and Davis, C. C., *Bioelectromagnetics* 4(1983)21-42
- [2]. Swicord, M. L. and Davis, C. C., *Biopolymers* 21(1982)2453-2460
- [3]. Swicord, M. L., Edwards, G. S., Sagripanti, J. L., and Davis, C. C., *Biopolymers* 22(1983)2513-2516
- [4]. Edwards, G. S., Davis, C. C., Swicord, M. L., and Saffer, J. D., *Phys.Rev.Lett.*53(1984)1284-1287
- [5]. Edwards, G. S., Davis, C. C., Saffer, J. D., and Swicord, M. L., *Biophys. J.*, 47(1985)799-807
- [6]. Davis, C. C., Edwards, G. S., Swicord, M. L., Sagripanti, J-S., and Saffer, J., *Bioelectrochem. Bioenerg.*
- [7]. Athey, T. W., Stuchly, M. M., and Stuchly, S. S., *IEEE Trans. on Microwave Theory and Techniques*, MTT-30(1982)82-87
- [8]. Stuchly, M. A., Athey, T. W., Samaras, G. M., and Taylor, G. E., *IEEE Trans on Microwave Theory and Techniques*, MTT-30(1982)87-92
- [9] Davis, C. C., and Lee, C-S, *Proc. 13th Annual Bioengineering Conf.*, K.R. Foster, Ed., pp. Philadelphia, Pa.
- [10]. Kraszewski, A., Stuchly, M. A., and Stuchly, S. S., *IEEE Trans. Instrum. Measur.*, IM-32,385-386,1983
- [11]. Stuchly, M. A., and Stuchly S. S., *IEEE Trans. Instrum. Measur.*, IM-29,176-183,1980
- [12]. Sagripanti, J-S., Swicord, M. L., and Davis, C. C., *Rad. Res.*,110,219-231, 1987
- [13]. Stuchly, M. M, Brady, M. M, Stuchly, S. S., and Gajda, G., *IEEE Trans. Instrum. Measur.*, IM-31,116-119, 1982
- [14]. Sagripanti, J-L., and Swicord, M. L., *Int. J. Radiat. Biol.*, 50, 47-50, 1986
- [15]. Vieira, J., and Messing, J., *Gene* 19, 259-268, 1982
- [16]. Sagripanti, J.-L., *Arch. Virol.* 82, 61-72, 1984
- [17]. Swicord, M. L., and Davis, C. C., *IEEE Trans. on Microwave Theory and Techniques* MTT-29, 1202-1209, 1981
- [18]. Maniatis, T., Fritsch, E. F., and Sambrook, J., *Molecular Cloning - A Laboratory Manual*, Cold Spring Harbor, 1982, p468.
- [19].21. Seidell, A., *Solubility of Inorganic and Metal Organic Compounds*. Vol. I, 4th ed. pp.

904, O. Van Nostrand Co., Princeton 1958.

[20]. Messinger Comey, A., A dictionary of chemical solubilities, pp. 132. Macmillan and Co., London, 1896.

[21]. Izatt, R. M., Christensen, J. J., and Rytting, J. H., Chemical Reviews 71, 439-481, 1971

[22]. Takagi, K, and Negishi, K., J. Phys. D: Appl. Phys., 15, 757-765, 1982

THE EFFECT OF MICROWAVES ON PLASMID DNA

A preliminary study [14] carried out at the FDA Center for Devices and Radiological Health had indicated that microwave exposure at 2450 MHz caused single- and double-strand breaks in plasmid DNA. We became involved in a further detailed investigation of this phenomenon, in particular with regard to careful dosimetry. This work has been reported in detail elsewhere [12], but the central methods used and results obtained will be described here. Our results indicate that the interaction of MW with purified DNA *in the presence of a small amount of copper* can lead to single as well as double strand breaks.

The fact that the absorption of microwaves by pUC8.c2 plasmid DNA had been previously characterized [4-6] determined our choice of the DNA species to study. E.coli strain HB 101 containing plasmid pUC8.c2 [15] was grown in superbroth medium with 24 μ g/ml of ampicillin to an optical density of 0.8 at 650 nm. At this time, amplification of plasmid was accomplished by incubating for 15h in the presence of 75 μ g/ml of chloramphenicol. Cells were collected by centrifugation, resuspended in 50 mM Tris, 50 mM EDTA, 25% sucrose, pH 8.0 and incubated for 10 min at room temperature with freshly prepared lysozyme (2 mg/ml). After adding 1 volume of 0.3% Triton X-100, 187.5 mM EDTA, and 150 mM Tris at pH 8.0, the bacterial DNA was pelleted by centrifuging for 1 hr at 81,500 \times g. The supernatant was diluted 1:2 and digested with RNase A (0.6 μ g/ml) for 10 min at room temperature. The sample was extracted 3 times with 1 volume of phenol-chloroform-isoamylalcohol (25-25-1) each time, as previously described [16], and phenol was removed from the aqueous phase by a final extraction with chloroform-isoamylalcohol (25:1). DNA was precipitated by adding 0.1 volume of 3M sodium acetate, pH 5.6, and 2 volumes of cold ethanol and kept either overnight at -20°C or 15 min at -70°C. After centrifuging for 15 min at 12,800 \times g, the sample was redissolved in 50 mM Tris, 10 mM EDTA, 500 mM NaCl, pH 7.5 and chromatographed through sepharose 4 B 1 \times 25 cm columns at 0.2 ml/min, with continuous monitoring of optical density at 260 nm with an Uvicord II (LKB, Stockholm, Sweden). The first peak containing the plasmid DNA was saved, and the second peak containing digested RNA was discarded. DNA was extracted again once with phenol and once with chloroform-isoamylalcohol and reprecipitated with ethanol. After lyophilizing the DNA in a rotary evaporator SpeedVac (Savant, Farmingdale, New York), it was redissolved in storage buffer (10 mM Tris, 10 mM NaCl, 1 mM EDTA, pH 7.5). Absence of

protein impurities was established spectrophotometrically, and DNA integrity was determined by agarose gel electrophoresis. The plasmid DNA was quantified spectrophotometrically with a Beckman Model 24 spectrophotometer. The accepted standard optical density (OD) at 260nm of 1 OD for 50 μg /ml of DNA [18] was used as the measurement standard. Only DNA samples with an OD 260/280 ratio between 1.85 and 2.00 and with no electrophoretically detectable degradation products were used.

Agarose gel electrophoresis (AGE)

One percent agarose gels were cast in 25 x 20 cm trays of a model H0 apparatus (Bethesda Research Laboratories, Gaithersburg, Maryland), allowing 20 samples to be analyzed simultaneously. Gel and electrode buffers were 41 mM Tris, 20 mM sodium acetate, 2 mM EDTA, pH 7.8. Samples were mixed with 0.25 volume of loading buffer (bromophenol blue 0.25%, sucrose 40%), loaded onto the gel and electrophoresed at 80V (80 mA) for 8 hr, a time in which the bromophenol blue used as a tracking dye migrated about 12 cm. A Hind III digest of Lambda phage DNA was always simultaneously run to provide a molecular weight standard. After the run, DNA was stained for 30 minutes with ethidium bromide (5 μg /ml), and the bands were visualized under UV light and photographed with Polaroid 665 positive-negative film. Negatives so obtained were measured densitometrically at 555 nm with a GS 300 densitometer (Hoeffer, San Francisco, California). The region of linearity between the amount of DNA in the gel and the optical density of bands in the electropherograms was experimentally established. All subsequent experiments were analyzed within this range of densitometric linearity.

Although plasmid DNA from commercial sources is well suited for transfection and other standard recombinant DNA techniques, its use in our experiments was avoided since the number of bands after AGE and the proportion of DNA in them made it difficult to determine DNA damage.

Chemicals

Restriction enzyme Pst I and Hind III digests of Lambda phage DNA were purchased from Bethesda Research Laboratories (Gaithersburg, Maryland). Lysozyme, CuCl_2 , and RNase A, as well as ampicillin and chloramphenicol were purchased from Sigma Chemicals (St. Louis, Missouri). In some of our experiments, the exposure antenna was coated with a thin layer of dielectric material. A convenient material for this purpose was finger nail polish (containing

nitrocellulose, formaldehyde resin, nylon and acrylate copolymer - cat 20 G, Maybelline, Litterock, Arkansas). The agarose used was from Sea Chem (Rockland, Maine), and CuCl was purchased from Mallinckrodt (Paris, Kentucky).

Exposure system

The exposure system is shown schematically in Fig.(9). MW are generated by a Hewlett Packard Model 8616A signal generator and conducted over a 15-decibel (dB), precision, high-directivity dual directional coupler (Wavecom, Model M-921, 1-12GHz) and a 10 -dB attenuator to a General Radio Model 900-LB precision slotted line. The output from the slotted line feeds an open-ended coaxial antenna immersed in the liquid sample. The open-ended antenna is made of standard 50 ohm, 3.58 mm outer diameter copper solid coaxial line with a 1 mm diameter center conductor and a composite polyethylene-teflon dielectric. The dielectric outer diameter is 2.96 mm. The open end of the antenna is machined flush and does not have either a protruding center conductor or an extended ground plane. The near field pattern of such an antenna has been described in detail previously [17]. Liquid samples were contained in 1.5 ml Eppendorf polypropylene micro test tubes into which the exposure antenna was immersed. Exposures were made in a continuous-wave mode with no amplitude modulation and frequency was continuously monitored with a Hewlett Packard 5340A frequency counter. Forward and reflected powers could be monitored with power meters (HP Model 435A, with HP Model 8481A power sensors). VSWR was measured with a VSWR meter (HP Model 415E). Sham exposures were identical to actual exposures insofar as the antenna remained immersed in the sample, but no microwaves were turned on.

Results

Microwave dosimetry

The small volumes of sample to be irradiated in our experiments make dosimetry difficult. Consequently, we used two different methods to set reliable upper and lower limits to the specific absorption rate (SAR) values used. By calibrating our dual-directional coupler and the attenuation of the system components with calibrated power sensors, we could accurately relate the forward power at the antenna to the recorded power from the dual-directional coupler shown in Fig.(9). Under exposure conditions, the voltage standing wave ratio (VSWR) in the system was measured. These measurements were made at low power to avoid saturation

Exposure System

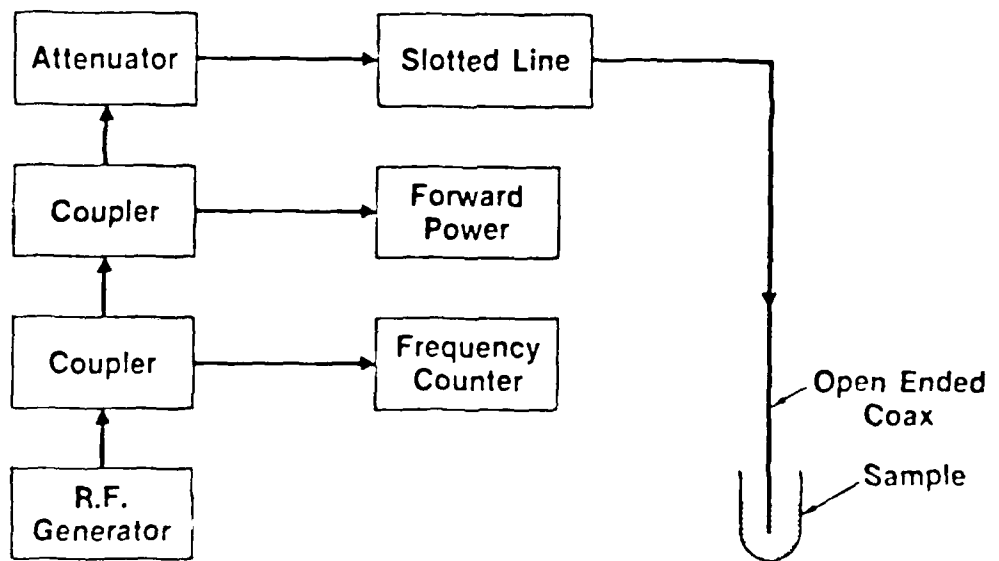


Fig. 9. Block diagram of the exposure system used for irradiating DNA samples.

effects and used minimal probe penetration in the slotted line. The fractional amount of forward power that is not reflected at the open antenna is then determined from the formula

$$T = 1 - [\tanh(r(\text{dB}) / 17.372)]^2$$

where $r(\text{dB})$ is the VSWR. Measured VSWR was insensitive to the volume of sample for sample volumes in the 20 - 100 μl range and corresponded to $T = 0.144 \pm 0.015$. If all the forward power P at the antenna is assumed to be absorbed in a sample of mass M then a maximum SAR (SAR_{max}) is determined from the formula

$$\text{SAR}_{\text{max}} = TP/M$$

Since some of the power is lost by passing right through the sample, the actual SAR (SAR_{true}) will be smaller than SAR_{max} .

To determine a minimum SAR (SAR_{min}), a Hughes Model 1177H amplifier was placed after the generator in Fig.(9) to boost the power applied to the sample. With a Vitek model 101 probe, the temperature rise ΔT of the sample as a function of time t could then be measured. SAR_{true} will be greater than this, because the thermal mass of the antenna, Vitek probe, and micro test tube reduces the observed $\Delta T/\Delta t$. The inserted volume of the probe in these experiments is about 2 μl so it is not the dominant thermal sink. We should point out that the Vitek probe was not immersed in the DNA samples during actual exposures, and was only used during dosimetric calibrations. Under the conditions of our experiment, we measured $\text{SAR}_{\text{max}} \sim 5 \text{ SAR}_{\text{min}}$. Obviously, $\text{SAR}_{\text{min}} < \text{SAR}_{\text{true}} < \text{SAR}_{\text{max}}$.

During microwave exposure, the electric field at the surface of the antenna can be calculated from the forward and reflected powers, and the annular area, A , between the inner and outer conductors of the coax. The maximum surface field results when all the power is reflected. In this case, the field, E , associated with the forward travelling wave is related to the forward power, P_{forward} , as follows:

$$P_{\text{forward}} = AE^2/(2Z)$$

where Z is the characteristic impedance of the coaxial line, 50 ohm in this case. The maximum

possible field at the antenna surface is

$$E_{\max} = 2(2ZP_{\text{forward}}/A)^{\frac{1}{2}}$$

For an annular area of $6.0 \times 10^{-6} \text{m}^2$ and a forward power of 0.28mW (corresponding to 10 mW/g for 28 μl of sample) the maximum surface field is about 136 V/m.

Characterization of the DNA sample

Plasmid pUC8.c2 DNA was analyzed by AGE under nondenaturing conditions. The DNA was incubated with various amounts of the restriction nuclease Pst I. This enzyme has a single cutting site in pUC8, which is the precursor of pUC8.c2 [17]. Low levels of enzyme present during short incubations produced mainly relaxed circles as a consequence of single strand breaks (Fig.(10), lanes 4 and 8). Further digestion resulted in total conversion into the linear form of the plasmid as a consequence of double strand breaks. Complete digestion of pUC8.c2 yielded the 2.7 kb linear form identical to the one obtained by digestion of pUC8 (lanes 11 and 6 respectively), indicating that pUC8.c2 consists of two pUC8 genomes linked together. Comparison with molecular weight standards in lane 1 permits the corresponding structures to be assigned to the remaining bands.

Effect of microwaves on DNA

Since our previous work had indicated a maximum absorption of microwaves at 2.55 GHz [14], we exposed 10 μg of plasmid DNA at this frequency for 20 min in 28 μl of storage buffer, using the exposure system shown in Fig.(9). To avoid any systematic errors, the DNA was divided into identical samples and randomly assigned to the different treatments (MW exposed or sham exposed). The order of the treatments was also randomized. Subsequent analysis of exposed DNA by AGE showed increased amounts of relaxed circular and linear DNA after MW exposure. Fig.(11) demonstrates the relaxation of DNA to be power dependent.

In 6 independent experiments at a SAR_{\max} of 10 mW/g, there was a significant difference ($P < 0.05$) in the number of double strand breaks produced between exposed and sham-exposed DNA. The percentage of linear DNA with respect to total DNA analyzed was 12.0 ± 2.6 and 4.6 ± 1.5 for exposed and sham exposed DNA, respectively (mean \pm standard error from six experiments). Periodic AGE analysis of DNA incubated at 8°C for up to two weeks after microwave exposure showed the damage produced after a single microwave exposure to be irreversible and not progressive.

Identification of Species in PUC8c2 By Restriction Mapping with PST I

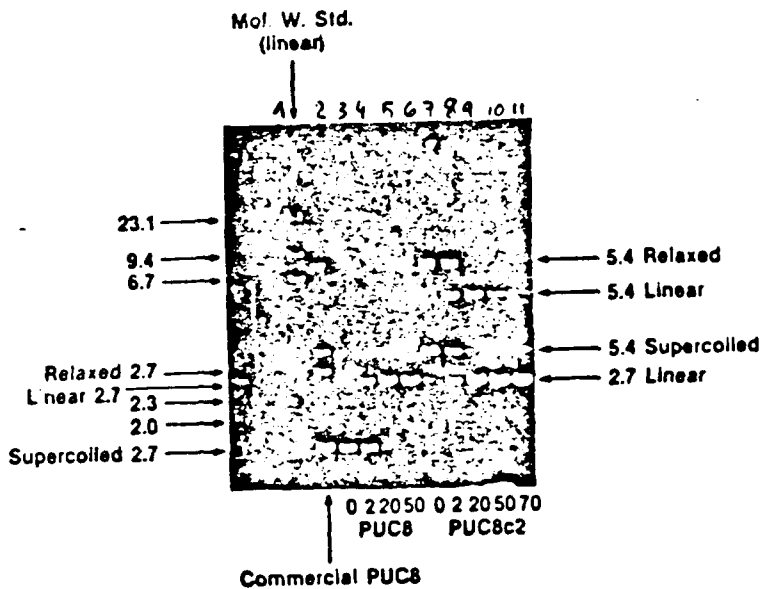


Fig. 10. Identification of species in pUC8.c2 plasmid by restriction mapping with Pst I enzyme. Plasmid DNA ($10 \mu\text{g}$) was digested with 0, 2, 20, 50 or 70 units of Pst I for 60 min at 19°C . Treated DNA was sampled on 1% agarose gel and electrophoresed 9 h at 80 V -80 mA. After staining with ethidium bromide, photographs were made. Commercial puC8 and puC8 prepared in our laboratory and digested with 0, 2, 20 and 50 units of Pst I are included for comparison. A Hind III digest of Lambda phage DNA, showing the linear subunits 23.1, 9.4, 6.7, 2.3, and 2.0 kb long is included as molecular weight standard (Mol. W. Std.).

Effect of Microwave Radiation on Plasmid DNA Structure

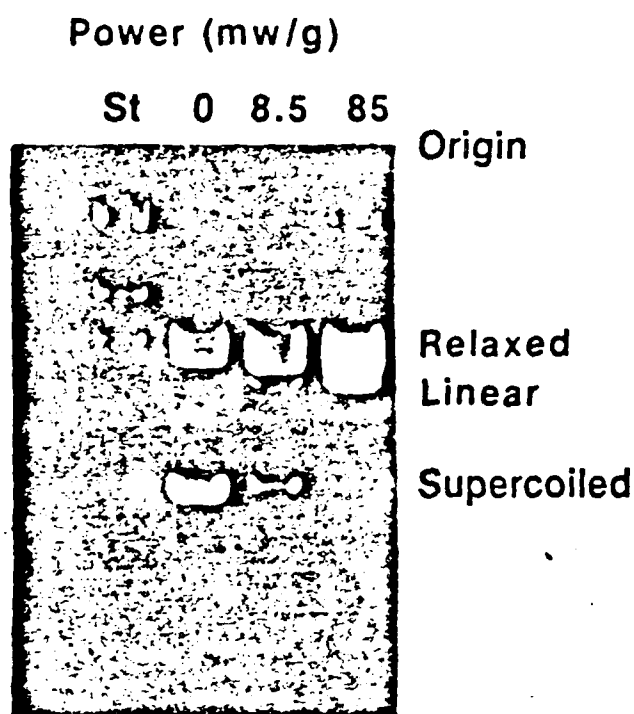


Fig. 11. Effect of microwave radiation on plasmid DNA structure. DNA was exposed for 20 min at 2.55 GHz at a SAR_{max} of 0, 8.5, and 85 mW/g before electrophoresis, as in Fig. 9. The gel was stained with ethidium bromide and photographed. A Hind III digest of lambda phage DNA was included as size standard (St).

Absence of sample heating

It should be noted that our maximum exposure levels are above the ANSI 1982 C.95 recommended exposure level of 0.4 mW/g. This does not *a priori* imply "thermal" exposure at higher levels. The ANSI standard was formulated, with a factor of 10 safety factor, to avoid exposure levels where any significant bioeffects had been observed, and this included systems whose thermal isolation prevented their being able to dissipate absorbed energy. In our experiments involving a half-hour exposure at 10 mW/g the maximum *possible* temperature increase of an isolated sample would be only 4°C.

Our samples had a large surface-area to volume ratio so they dissipated absorbed microwave energy efficiently. Under exposure conditions corresponding to a SAR_{max} of 10 mW/g we could not detect any heating over and above typical ambient temperature drifts (typically $\pm 0.1^\circ\text{C/hr.}$). In this sense our exposures are *athermal*. To detect any significant temperature increase in our samples we had to use exposure levels on the order of 1 W/g, as shown in Fig.(12). This is a SAR level at least two orders of magnitude higher than the maximum used in our experiments (<10mW/g). To find out whether relaxation of DNA under our experimental conditions was sensitive to small temperature increases, plasmid DNA samples were incubated at various temperatures and the strand breaks produced compared with sham and microwave exposed DNA. Fig.(13) shows that raising the temperature of the sample by 8°C does not produce any significant difference from the sham exposed DNA, while microwave-exposed DNA shows an increased amount of both relaxed circular and linear DNA. In other experiments, an increase in the temperature of our DNA samples even by 30°C above room temperature did not cause the damage observed after MW irradiation.

Characteristics of the effect

To determine whether the microwave effects on DNA had any frequency specificity, we selected several different frequencies, including those shown previously to correspond to resonant absorption (2.55 and 8.75 GHz) or minimum absorption (2.00, 3.45 and 7.64 GHz) of MW by DNA. We could not detect any significant variation in double strand break formation attributable to resonant absorption of the DNA at specific frequencies (data not shown).

To support our data statistically, results from 12 independent experiments at the five frequencies stated above are pooled and summarized in Fig.(14). Again microwave exposed

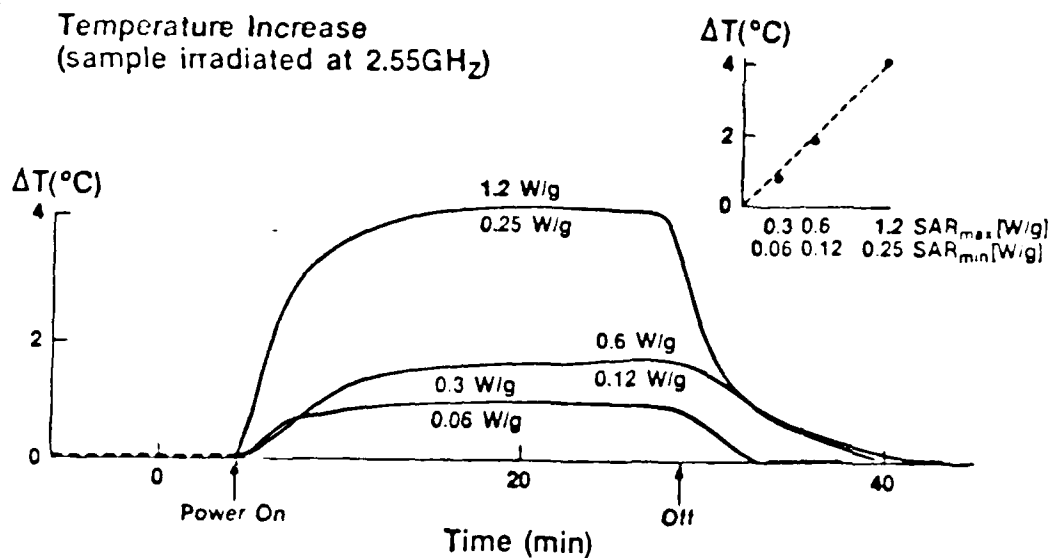


Fig. 12. Time history of temperature increase in samples irradiated at high values of SAR. A value of SAR_{min} is determined from the initial slope of the heating curve. The figures above and below each curve are the corresponding SAR_{max} and SAR_{min} , respectively, in each case. The power had to be boosted to Watt per gram levels into a 0.1 ml sample in order to record temperature increases.

Effect of Temperature on Plasmid DNA

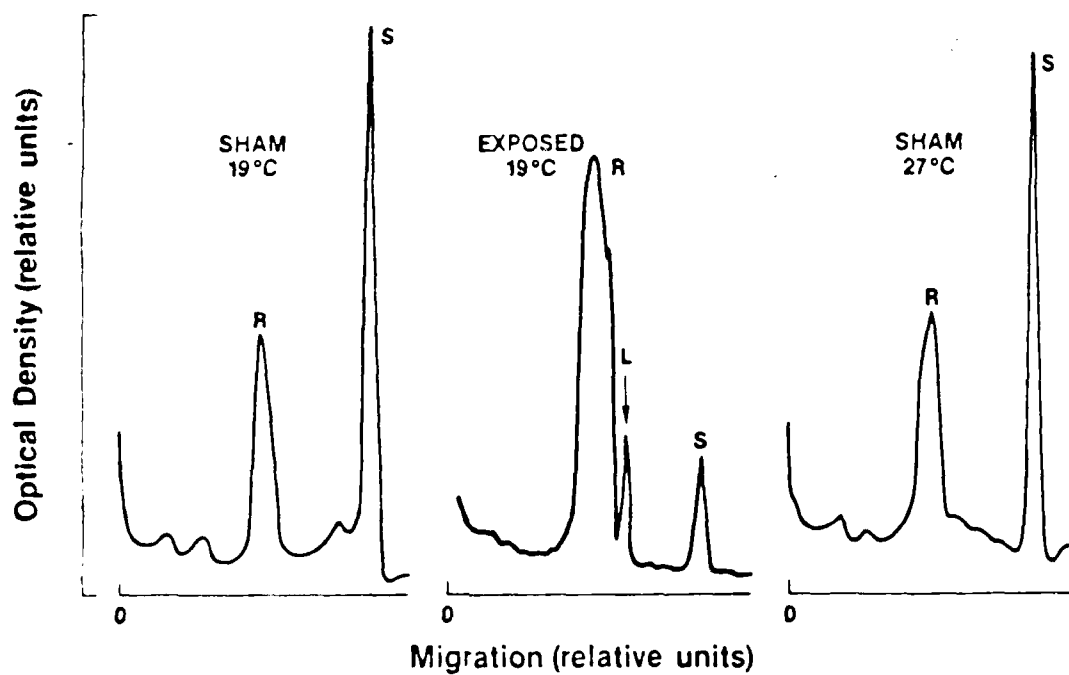


Fig. 13. Effect of temperature on plasmid DNA. DNA was sham exposed at 19°C, incubated at 27°C or exposed at 19°C at 10 mW/g; treatment duration was 20 min. Photographs were taken of the electrophoresis gels and the densitometry of the negatives is shown. Electrophoresis is from left to right. The peaks correspond to DNA: supercoiled (S); linear (L); and relaxed (R).

Summary of DNA Double Strand Break Formation N Observations in E Experiments

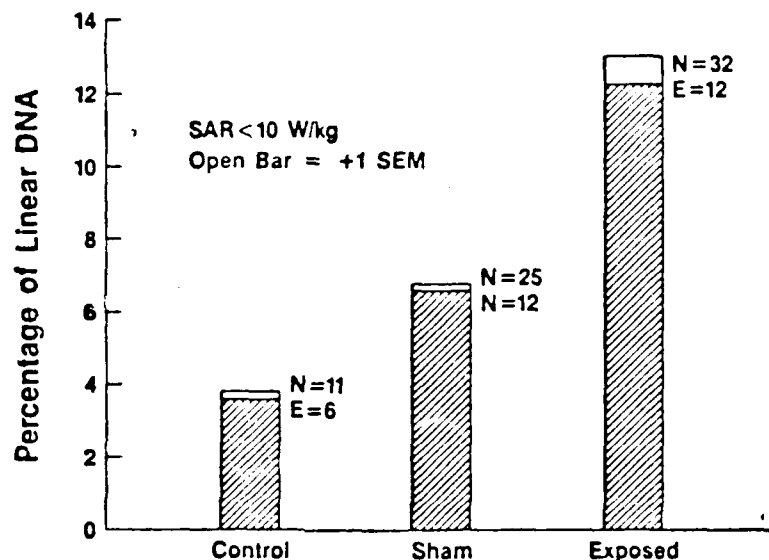


Fig. 14. Summary of DNA double strand break formation. Data taken at frequencies from 2 to 8.75 GHz were pooled and statistically analyzed together. Legends indicate DNA exposed at a SAR_{max.} of 10 mW/g (Exposed), sham exposed at 0 mW/g (Sham) or control DNA kept close but in no contact with the antenna (Control). Different DNA species were quantified as in Fig. 13. Mean and standard error of the percentage of linear DNA with respect to the total DNA in the sample obtained in N observations from E independent experiments is displayed.

DNA showed more breaks than sham irradiated DNA. Interestingly here, sham exposed DNA exhibited a significantly higher level of double strand breaks than unexposed control DNA kept close to, but in no contact with, the copper antenna.

Fig.(15) shows the results of a kinetic study of the production of double strand breaks in sham exposed DNA and DNA exposed at 8.75 GHz for different times at an SAR_{max} of 10 mW/g. There are about seven times as many double strand breaks observed in MW exposed DNA at a level of 10 mW/g at 8.75 GHz compared with sham exposed DNA. Also a control sample of DNA was analyzed. These experiments showed again that sham exposed DNA in contact with the copper antenna, but with the MW switched off, consistently suffered more damage than control DNA.

Participation of copper

Since the only difference between sham and control DNA was contact of the former with the copper antenna, the participation of copper in the process of DNA breakage was further studied. Identical results to those just described were obtained when just before the experiment, the copper antenna was sterilized by autoclaving or any trace of oxide was removed by immersing it in 0.5 N nitric acid. When the antenna was covered with a thin plastic coating, controls and shams became indistinguishable, with complete elimination of DNA breakage. With the coated antenna, the effect of MW on DNA also became undetectable. The incubation of DNA with cuprous but not cupric ions, in the absence of MW or antenna contact, mimicked the damaging effects observed after MW radiation with the copper antenna (Fig.16)).

One phenomenon that could, perhaps, explain some of our observations is partial rectification of the MW field at the outer surface of the antenna, leading to electrolysis, or some other mechanism which caused increased amounts of copper to pass into solution when the microwaves were turned on. Since the amount of copper expected to be present in our samples is exceedingly small, the possibility of MW-mediated electrolysis can only be tested indirectly. To test whether such phenomena might be important, we exposed DNA samples to a low frequency field (10 kHz) at field strengths at the uncoated antenna surface of up to 4500 V/m. These surface electric fields, which are radially directed between the inner and outer conductors at the open end of the coaxial antenna, are several times larger than the fields present during any of our MW exposures. For a SAR_{max} of 10 mW/g the maximum possible surface field is 136 V/m. Electrolytic effects, if they occur, should depend on the strength of

Microwave Induced Double Strand Breaks

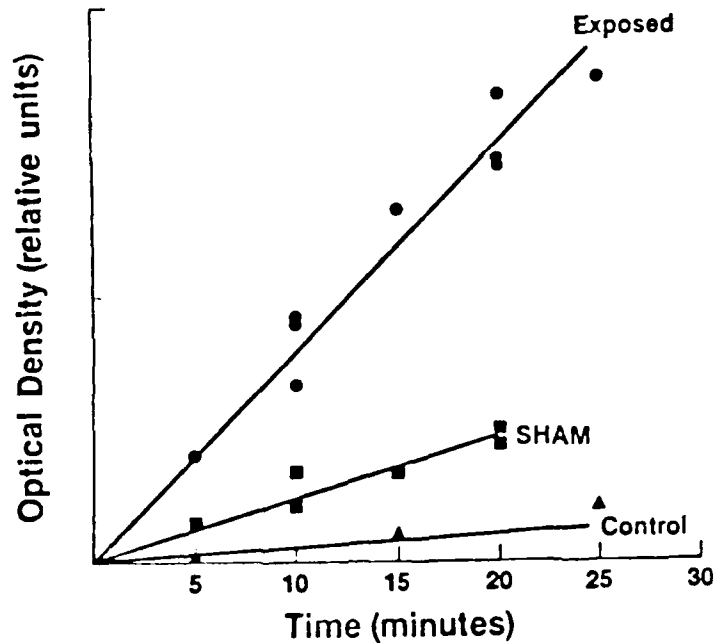


Fig. 15. Kinetics of double strand break formation resulting from microwave exposure. Plasmid DNA was exposed at a SAR_{max} of 10 W/kg at 2.55 GHz during the time periods shown in the figure (exposed ●—●). Sham irradiated samples were identical to exposed except that the power was switched off (■—■). Control DNA samples were identical to sham irradiated DNA except that sample was close to but not in contact with the copper coaxial antenna (▲—▲). After exposure, samples were electrophoresed, and the amount of linear DNA produced was obtained after densitometry as in Fig. 13.

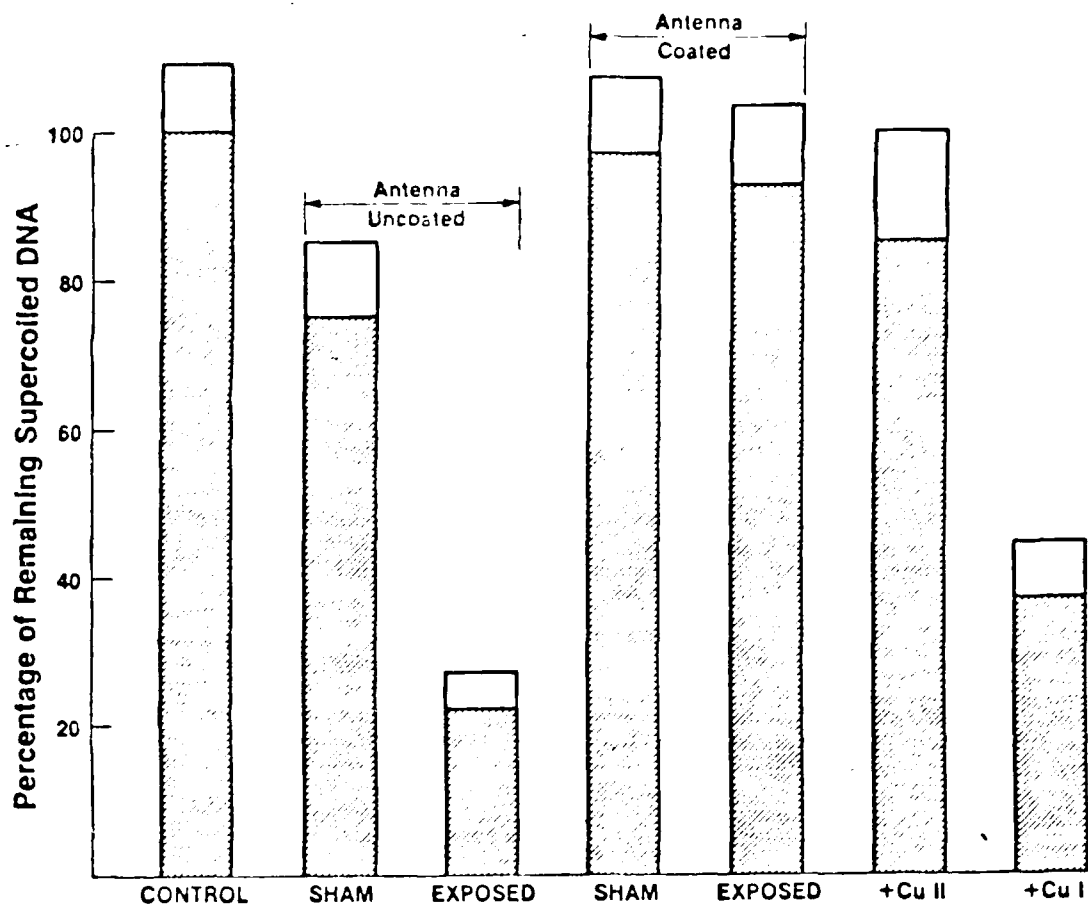


Fig. 16. Total damage produced in DNA as measured by the remaining supercoiled DNA. DNA was sham exposed or exposed at 2.55 GHz for 20 min either with an uncoated copper or plastic coated antenna. Separate samples not in contact with any antenna were incubated for equal times either in storage buffer (CONTROL), cupric chloride at a final concentration of 10 mM (Cu II), and cuprous chloride (Cu I) at saturation, which is about 0.6 mM⁽²⁴⁾. Analysis was done by AGE and in each case the mean of three experiments \pm the standard deviation is displayed

the fields at the copper electrode surface and should be enhanced at lower frequencies. The results (Fig.(17)) show that even at a field strength of 4500 V/m these lower frequency fields do not produce the DNA damage caused by exposure to MW. We believe this rules out any unexpected electrolysis effects in explaining our observations.

Discussion

Contact with the copper antenna produces slight but noticeable damage to isolated DNA. MW significantly increase such damage. The effect of MW is to increase the number of single and double strand breaks. The damage is linearly related to both the power applied and the duration of the exposure to MW.

Effects on DNA were observed throughout the frequency range studied and could not be correlated with resonant frequencies previously reported [4-6]. However, the sensitivity required for detecting any resonant effects may well be out of the range of the technique used here. At this stage of our work we do not think that excitation of a specific internal vibrational mode of the DNA explains our observations.

Temperature increase seems to play no role in producing the breaks, since no temperature increase was actually measured in the irradiated sample, and no significant heating is predicted from our calculations. The large thermal mass of the antenna relative to the sample has two main advantages. First, the antenna is an effective heat sink. Second, the immersion of an antenna 3.5 mm in diameter made the 28 μ l sample adopt a hemispherical conformation of similar radius to that of the antenna. Calculations have shown that there are no "hot-spots" of the field in this irradiation geometry [17]. Indeed, the maximum point SAR possible in the sample cannot be much greater than twice the average values obtained from our dosimetry measurements. MW heating does *not* produce the effects reported here. This is further supported by the fact that raising the temperature of the sample several-fold over any possible increase due to our MW exposure did not produce any damage to the DNA.

Surprisingly, metal ions appear to play a significant role in the interaction of MW with DNA. The solubility of copper in water is 160 μ g/l [19] and dissolution of as much as 17 μ g of copper per dm² per hr of contact of solid copper with distilled water has been reported [20]. If only one-tenth of this amount is dissolved in our buffer (which also contains 20 mM salt and 1 mM EDTA, and could therefore be a better solvent than water) during the short time of

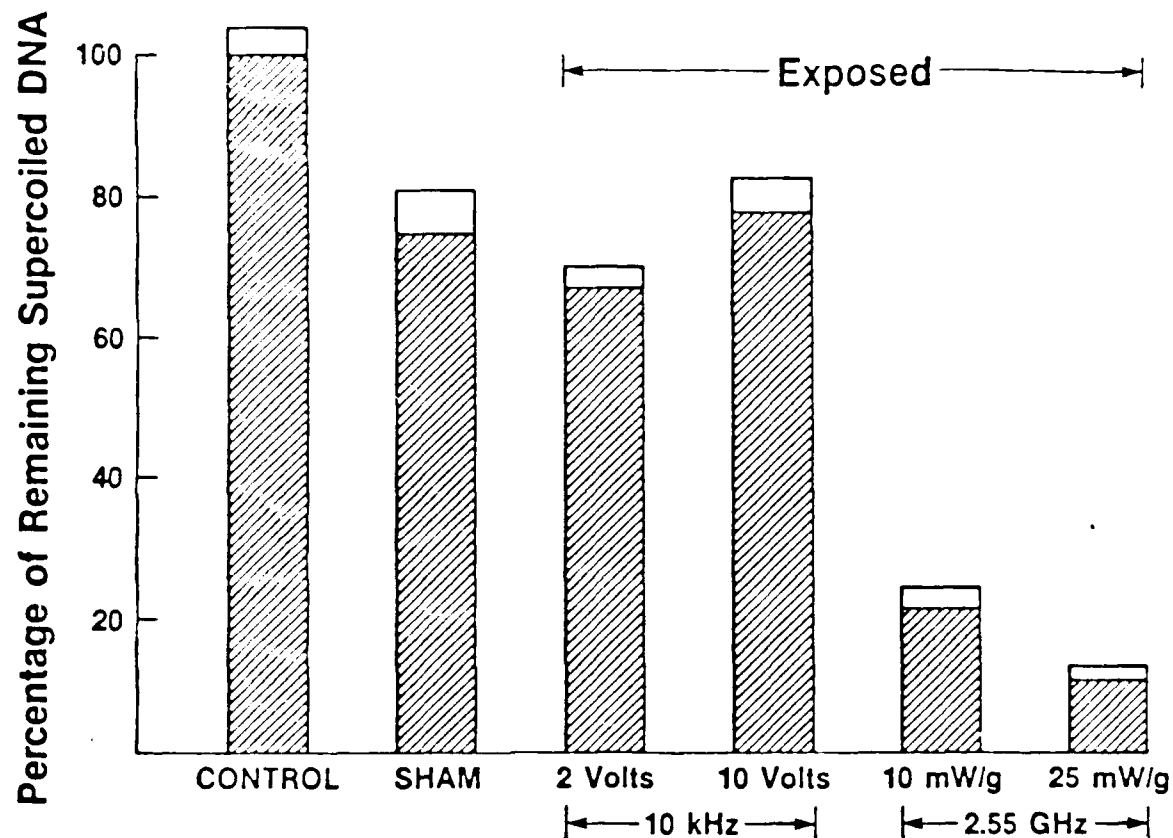


Fig. 17. Comparison between effects of exposure of DNA at 10 kHz and 2.55 GHz. Plasmid DNA was exposed for 15 min with an uncoated copper coaxial antenna at a frequency of either 10 kHz or 2.55 GHz at the levels stated in the Figure. Sham irradiated samples were identical except that both power sources were switched off. The result for control samples kept close to, but not in contact with, the antenna is shown for comparison. After treatment, samples were analyzed by AGE, photographed and optical densities obtained. The height of the bars indicates the mean values obtained in two independent experiments with two replicates each; empty bars indicate the standard deviation of these results.

exposure, there are still about 2 molecules of copper per molecule of plasmid DNA expected to be present in our samples. This fact alone should sound a note of caution in interpreting any previous reports about MW effects in which the experimental sample was in contact with a metallic antenna. Cuprous ions mimic the damage to DNA produced by MW and the copper antenna, suggesting that this ion plays an intermediary role in producing the strand breaks.

Any electrolytic effect produced by MW is very unlikely. This is demonstrated by our observation that a large, 10 kHz modulated surface field did not reproduce the damage to DNA produced by MW irradiation. This suggests that copper ions are present in both shams and exposed samples, presumably at the same low concentration determined by the solubility of the copper present in the antenna.

Since metal ions bind tightly and specifically to biomolecules, especially nucleic acids [21], any interaction of MW with metal ions will be likely to affect the macromolecule. It is unclear to us at present what specific mechanism is responsible for the observed synergistic interaction between copper ions and microwave irradiation in producing DNA damage. However, the fact remains that for identical sham and MW irradiated DNA samples, the MW exposed samples show significantly more breaks than the nonexposed. Certainly, the microwaves can excite internal motions of the DNA which might, if the motional amplitudes were sufficiently great, allow metal ions more access to a reactive site. There is still the possibility that through some rectification at a heterogeneous interphase at the molecular level, a local electric potential is shifted enough to alter the balance of some electrochemical processes and lead, for example, to free radical formation. However, such mechanisms are at present speculative. The irradiation levels used in our experiments are so low that the average increase in excitation level per molecule does not, in a simple way, explain how a process with any significant activation energy could occur.

It is hoped that by pursuing these studies a mechanism of interaction between MW and biological systems will arise. Such a mechanism is needed for clarifying the controversial issue of MW bioeffects and for assessing any risk associated with them. The ability of an agent to cause single strand breaks as well as more potentially harmful double strand breaks, is generally related to mutagenesis and carcinogenesis. However, the fact that this work was done exclusively in vitro with pure DNA molecules should be kept in mind in any attempt to extrapolate our observations to more complex living systems.

ULTRASONIC ABSORPTION STUDIES OF BIOMATERIALS

There are frequently common features to the dielectric and ultrasonic behavior of materials. Electromagnetic field excitation leads to the alignment of polar molecules and their subsequent orientational relaxation. This orientational relaxation takes place within the local environment of other molecules and involves dipole-dipole interactions and the viscosity of the solution. When an ultrasonic wave passes through a material, molecules are displaced from their equilibrium positions and subsequently relax. This relaxation is influenced by dipole-dipole interactions and the viscosity of the solution. In principle, both electromagnetic and ultrasonic stimulation can lead to the excitation of internal modes of molecules. Therefore, we have begun to investigate the ultrasonic absorption properties of various liquids to see if any features observed by dielectrometry can be observed ultrasonically. In particular we wished to see if any of the microwave absorption characteristics of plasmid DNA could be observed ultrasonically. A unique aspect of this work is that it brings together two unusual capabilities: the production of "customized" DNA solutions for study, and the availability of very high frequency acoustic transducers which have been designed for this work.

Experimental Method

While a variety of experiments has been conducted or considered, all experiments involve the use of high frequency ultrasonic transducers with responses extending to about 2 GHz. These transducers are made by thick platelet LiNbO_3 technology, with ion beam milling used for final transducer thinning.

Acoustic Transmission

When the first pair of operating transducers was finished, an attempt was made to observe acoustic transmission through an aqueous solution and to measure the acoustic attenuation of that solution. These experiments were conducted in the 100-400 MHz frequency range, since the two devices had not yet undergone ion beam milling to achieve final high center frequency. Also, since the acoustic attenuation of water, higher than most crystals to begin with, increases with the square of frequency, there was a better chance of observing a transmitted signal at lower frequency.

The acoustic attenuation of aqueous solutions, and also of ethanol, was successfully measured using the apparatus shown schematically in Fig (18). Results for a particular buffer

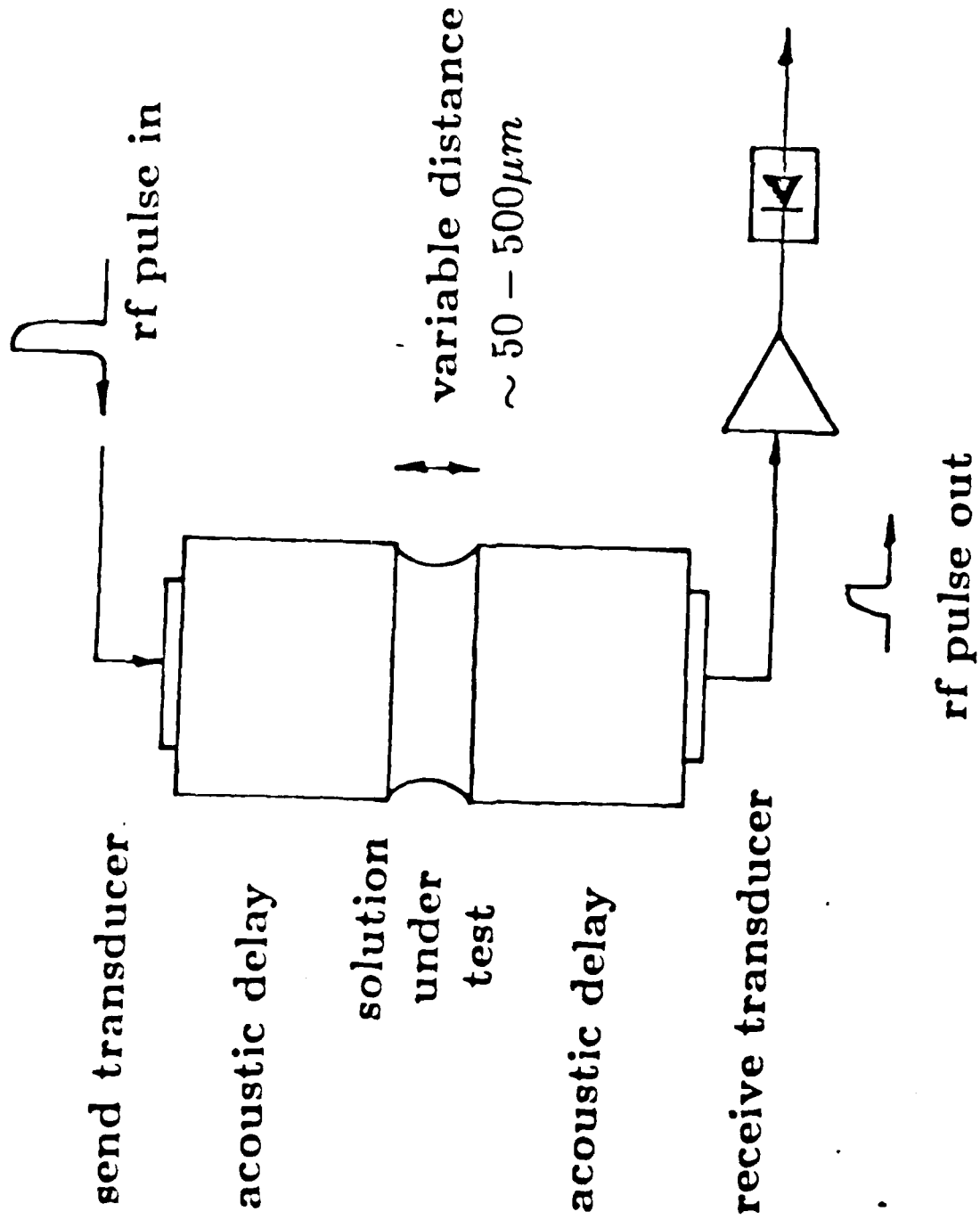


Fig. 18. Arrangement used in initial experiments to measure acoustic attenuation of liquids at microwave ultrasonic frequencies.

solution are given in Fig.(19). About 10% accuracy was achieved. As has been noted by previous investigators (the attenuation of pure water has for many years been used as a standard), this send/receive method is difficult to execute with great accuracy in this frequency range. Many experimental sources of error must be dealt with, including acoustic diffraction and temperature. It was not possible to distinguish reliably between pure water, DNA solutions, saline solutions, or buffer solutions using this technique.

We have begun to construct a more accurate system for measuring the ultrasonic properties of liquids using the optical heterodyne Bragg scattering method described by Takagi and Negishi [22].

END

DATE

FILMED

3 - 88

DTIC